Electronic Supplementary Material (ESI) for Energy & Environmental Science

Lone Pair Electrons Minimize the Lattice Thermal Conductivity
Supplementary information

Michele D. Nielsen[1], Vidvuds Ozolins[2,*] and Joseph P. Heremans[1,3,*]

1. Department of Mechanical and Aerospace Engineering, Ohio State University, Columbus, Ohio, USA
2. Department of Materials Science and Engineering, University of California, Los Angeles, USA
3. Department of Physics, Ohio State University, Columbus, Ohio, USA

1. X-ray diffraction (XRD) data

XRD data on all samples are reported in Fig. S1; all index to rocksalt structures, except for trigonal $AgBiSe_2$. No reference data were found for $NaBiTe_2$.

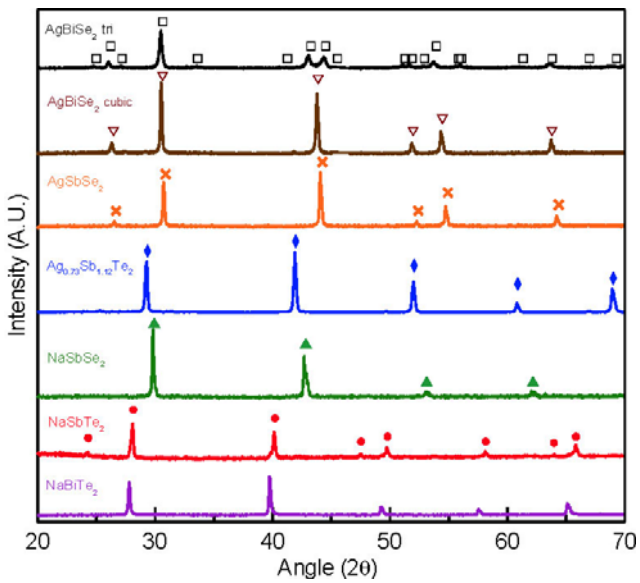

Figure S1: *X-ray diffraction data on the compounds prepared for this study. Except for $AgBiSe_2$, which was prepared in both its trigonal and rocksalt form by varying the heat treatment, all samples index in the NaCl structure. The dots are reference peaks from the International Centre for Diffraction Data PDF database.*

The lattice parameters of the $Ag_{1-x}Na_xSbTe_2$ alloys, shown in Fig. S2, follow a linear dependence on x, consistent with Vegard's law.

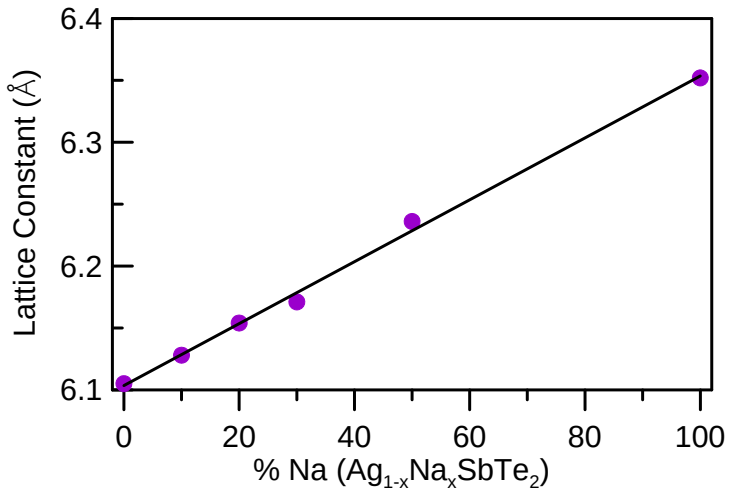

Figure S2: *The lattice parameter (in the rocksalt unit cell) of $Ag_{1-x}Na_xSbTe_2$ alloys as a function of composition.*

We show typical temperature-dependent X-ray diffraction data in Fig. S3.

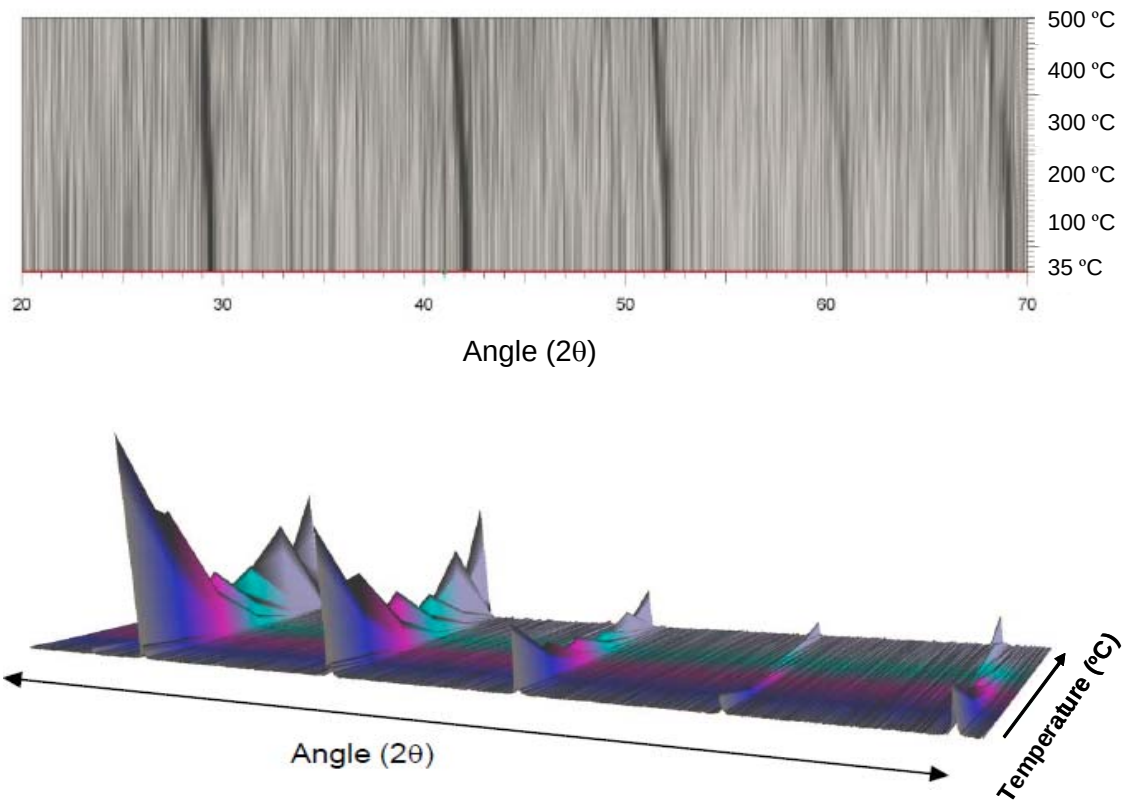

Figure S3 *Typical temperature-dependent X-ray spectra of measured cubic compounds.*

From these, the temperature-dependent lattice parameter can be calculated. The results are plotted Fig. S4: the lattice parameter increases linearly with *T*, so a single isotropic linear thermal expansion α can be derived and is reported in Table 1 (main text). The data reported for the nominal composition $AgSbTe_2$ were in fact obtained on $Ag_{0.73}Sb_{1.12}Te_2$.

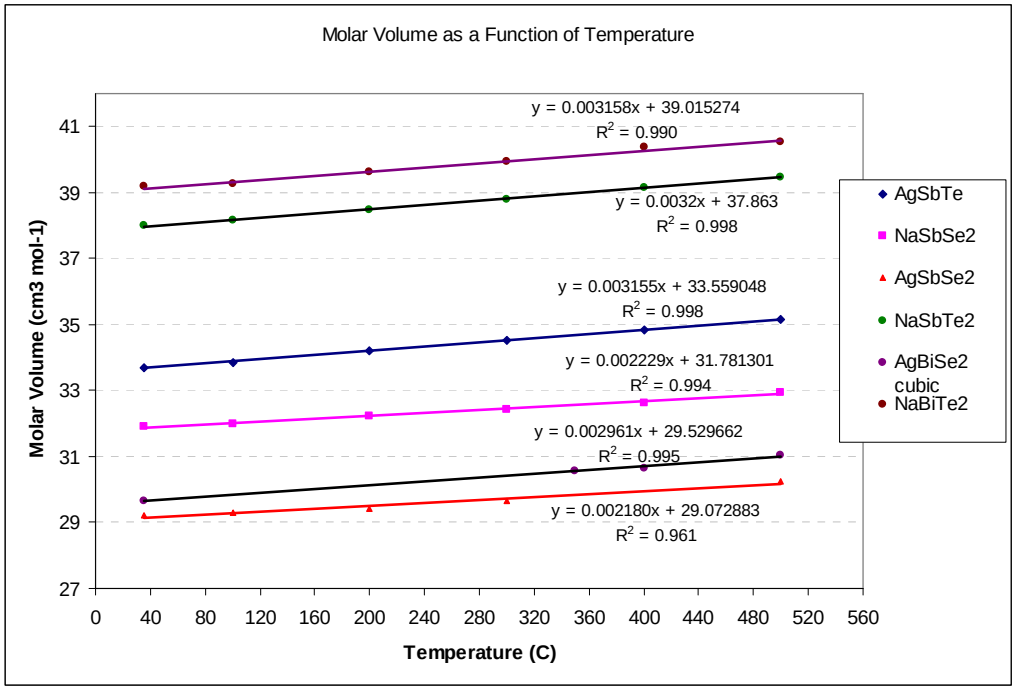

Figure S4 *Temperature-dependence of the lattice parameter calculated from data like Fig. S3. The linear thermal expansion coefficients α are calculated from the slope of these curves.*

2. Electrical properties

The electrical resistivity of most compounds studied experimentally is shown in Fig. S5. $NaSbSe_2$ is too electrically insulating to be measured. Except for $NaSbTe_2$, all compounds behave like semiconductors; $NaBiTe_2$ behaves like a doped one. Consistently with previous results on $AgSbTe_2$,[1] $Ag_{0.73}Sb_{1.12}Te_2$ behaves like a very narrow-gap semiconductor. All this implies that the density of native defects, to the extent that they act as donors or acceptors, is limited to sub-percentage levels.

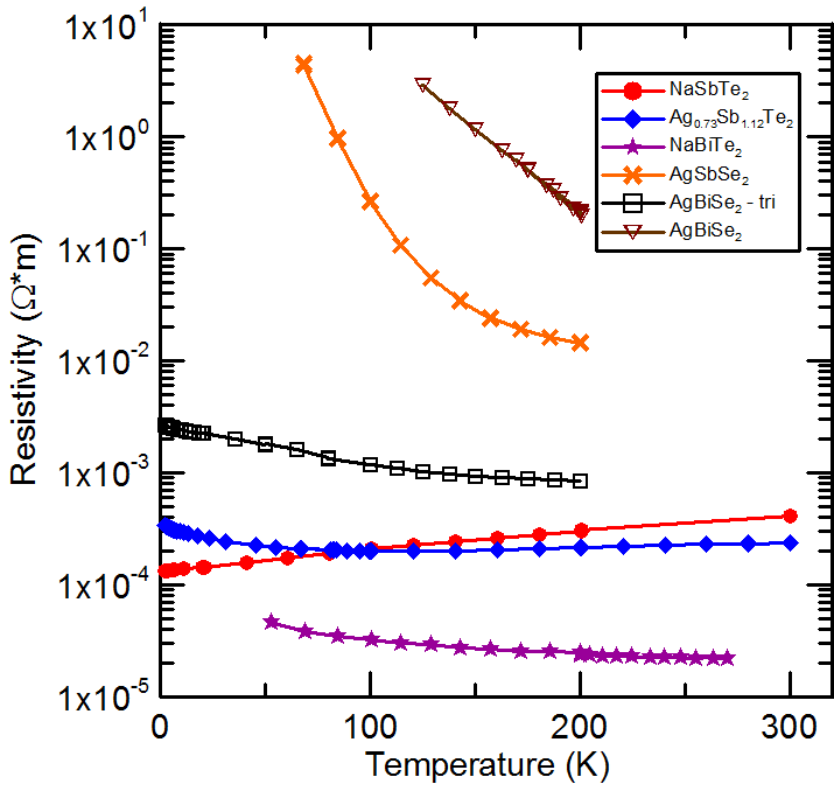

Figure S5: *Electrical conductivity of $NaSbTe_2$, $Ag_{0.73}Sb_{1.12}Te_2$, $NaBiTe_2$, $AgSbSe_2$, $AgBiSe_2$ (trigonal), and $AgBiSe_2$ (cubic). $NaSbSe_2$ was electrically insulating.*

[1] V. Jovovic and J. P. Heremans, Energy Band Gap and Valence Band Structure of $AgSbTe_2$, Phys. Rev. B **77** 245204 (2008)

3. Calculated phonon spectra: summary

The calculated phonon dispersions are reported in sections 5 and 6. From them, mode-averaged Grüneisen parameters γ, sound velocities and the zone edge energies, expressed as Debye temperatures Θ_i can be derived and tabulated in Table S1. Select data were reproduced in Table 1 of the main text. Lattice parameters a and bulk moduli B were calculated from the variation of the total energy vs. volume $E(V)$ by fitting the calculated points to 3rd-order polynomials in V.

Table S1. *The interatomic spacing (a/2), calculated bulk modulus B, mode-and-frequency averaged Grüneisen parameter γ, sound velocities, and zone-boundary Debye energy $k_B\Theta_i$ for phonons along the axes indicated.*

Theory	*a/2*	B	γ	Sound velocities(m/s)			Zone-boundary energy Θ_i (K)		
	(nm)	(GPa)		Gamma-to-X [x 0 -x]			X [¾ 0 -¾]		
				TA1	TA2	LA	TA1	TA2	LA
$NaSbSe_2$	0.2906	44	1.7	2132	2770	4329	76	89	114
$NaSbTe_2$	0.3103	35	1.6	1664	2430	3630	63	85	94
$NaBiTe_2$	0.3138	34	1.5	1295	2055	3131	40	56	56
				Gamma-to-K [0 x x]			K [0 ¾ ¾]		
				TA1	TA2	LA	TA1	TA2	LA
$AgSbSe_2$	0.2819	78	3.5	1362	2105	3433	47	52	62
$AgSbTe_2$	0.2972	67	2.3	1325	2469	3526	53	56	65
$AgBiSe_2$	0.2893	74	2.5						
$AgBiTe_2$	0.3018	66	2.5	1278	2116	3223	47	47	55

Note that the Debye temperature values Θ_D fitted to the specific heat (Table 1) are nearly twice the Debye temperatures Θ_i calculated from the zone-boundary acoustic phonon energies $k_B\Theta_i$ in Table S1. Two factors contribute to this. Firstly, there is a contribution of the optical modes to the high-temperature value of C. Secondly, Fig. 2 of the main text shows that many acoustic modes do not have monotonic energy-momentum relations, so that the maximum phonon energy is higher than the energy $k_B\Theta_i$ at the zone boundary.

The calculated mode-averaged Grüneisen parameters for all 72 compounds (8 Group I cations × 3 Group V cations × 3 Group VI anions) are given in Table S2 below.

Table S2: *Calculated mode-averaged Grüneisen parameters γ for all 72 compounds grouped by the group I cation. Higher γ values (stronger anharmonicity) correspond to warmer colors. Red squares indicate that the compounds have unstable phonon modes at the calculated equilibrium lattice parameter. $AgSbSe_2$ is predicted to have a weakly unstable L-point TA mode, and is found experimentally to have the lowest thermal conductivity of all materials considered in our study.*

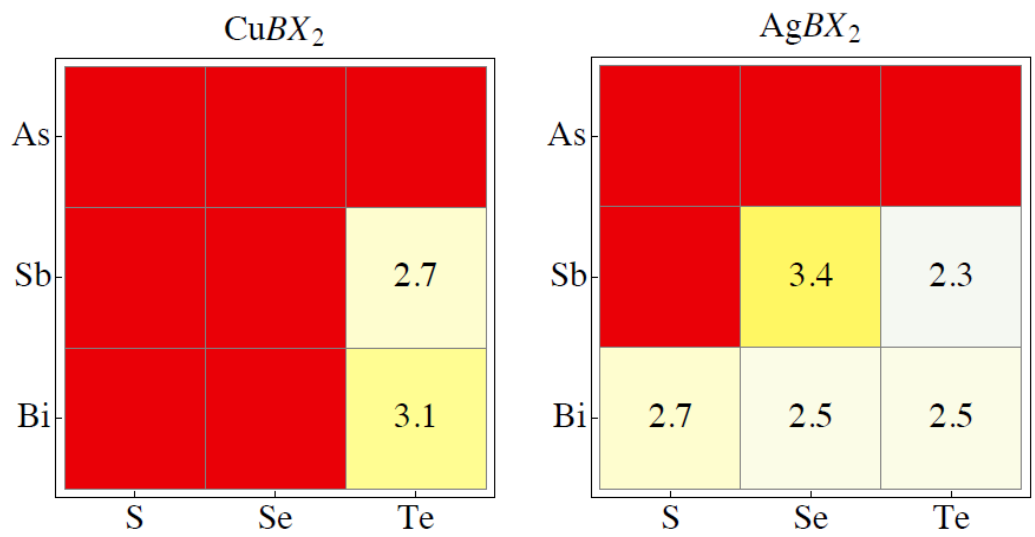

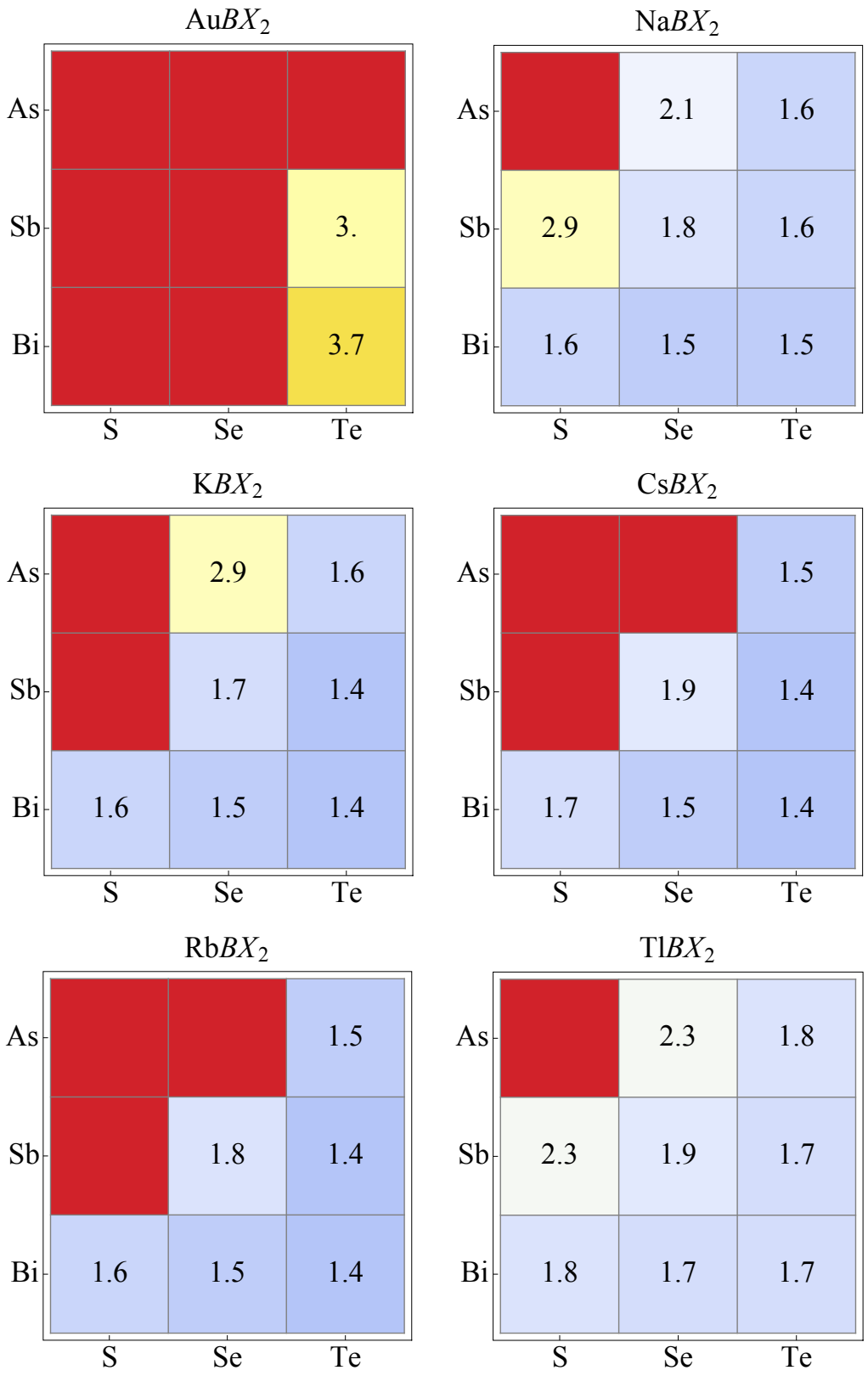
AuBX2
As
Sb
Bi
3.
3.7
S
Se
Te
NaBX2
2.1
1.6
2.9
1.8
1.6
1.6
1.5
1.5
KBX2
2.9
1.6
1.7
1.4
1.6
1.5
1.4
CsBX2
1.5
1.9
1.4
1.7
1.5
1.4
RbBX2
1.5
1.8
1.4
1.6
1.5
1.4
TlBX2
2.3
1.8
2.3
1.9
1.7
1.8
1.7
1.7

4. Literature with structural information of known ABX_2 compounds.

In agreement with our calculations, the crystal structures of several of the ABX_2 compounds have been determined experimentally and found to be either not rocksalt based or resemble highly distorted variants of rocksalt. The references are:

$CuSbS_2$: Razmara, M.F.; Henderson, C.M.B.; Pattrick, R.A.D. Mineralogical Magazine **61**, 79-88 (1997)

$CuBiS_2$: Portheine, J.C.; Nowacki, W. Zeitschrift fuer Kristallographie, Kristallgeometrie, Kristallphysik, Kristallchemie **141**, 387-402 (1975);

$CuSbSe_2$: Imamov, R.M.; Pinsker, Z.G.; Ivchenko, A.I. Kristallografiya **9**, 853-856 (1964);

$AgSbS_2$: Effenberger, H.; Paar, W.H.; Topa, D.; Criddle, A.J.; Fleck, M. American Mineralogist **87**, 753-764 (2002);

$NaAsS_2$: Palazzi, M.; Jaulmes, S. Acta Cryst. B **33**, 908-910 (1977);

$KSbS_2$: Graf, H.A.; Schaefer, H. Zeitschrift fuer Anorganische und Allgemeine Chemie **414**, 211-219 (1975);

$CsSbS_2$: Kanishcheva, A.S.; Mikhailov, Yu.N.; Kuznetsov, V.G.; Batog, B.N. Doklady Akademii Nauk SSSR **251**, 603-605 (1980);

$RbAsSe_2$: Sheldrick, W.S.; Haeusler, H.J. Zeitschrift fuer Anorganische und Allgemeine Chemie **561**, 139-148 (1988);

$RbSbS_2$: Kanishcheva, A.S.; Kuznetsov, V.G.; Lazarev, V.B.; Tarasova, T.G. Zhurnal Strukturnoi Khimii **18**, 1069-1072 (1977)

Rocksalt $CuBiSe_2$, $AgAsSe_2$, $AgSbSe_2$: Zhuze, V.P.; Sergeeva, V.M.; Shtrum, E.L. Soviet physics - Technical physics **3**, (10) 1925-1938 (1958); Tomaszewski, K. Phase Transition 38, 127-220 (1992); Geller, S.; Wernick, J.H. Acta Crystallographica 12, 46-54 (1959).

5. Calculated phonon spectra of the rocksalt compounds

The Brillouin zone of the rocksalt compounds, with the atomic arrangement of Fig. 1a, is shown in Fig. S6. The calculated phonon dispersions of rocksalt compounds follow with the compound name indicated above each panel. Compounds with spectra that contain imaginary calculated frequencies are not shown, with the exception of $AgSbSe_2$, which has been synthesized in the cubic structure in this study and in previous ones (Ref. 13 of the main text).

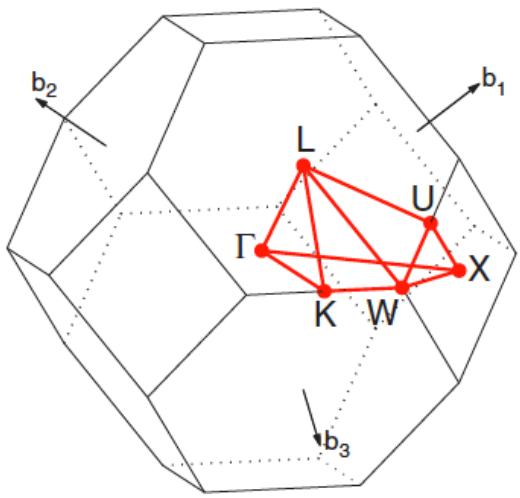

Figure S6. *Brillouin zone of cubic D4 (AF-IIb), and phonon dispersions of the stable noble metal D4 rocksalt-based ABX_2 compounds with A=noble metal (see below)*

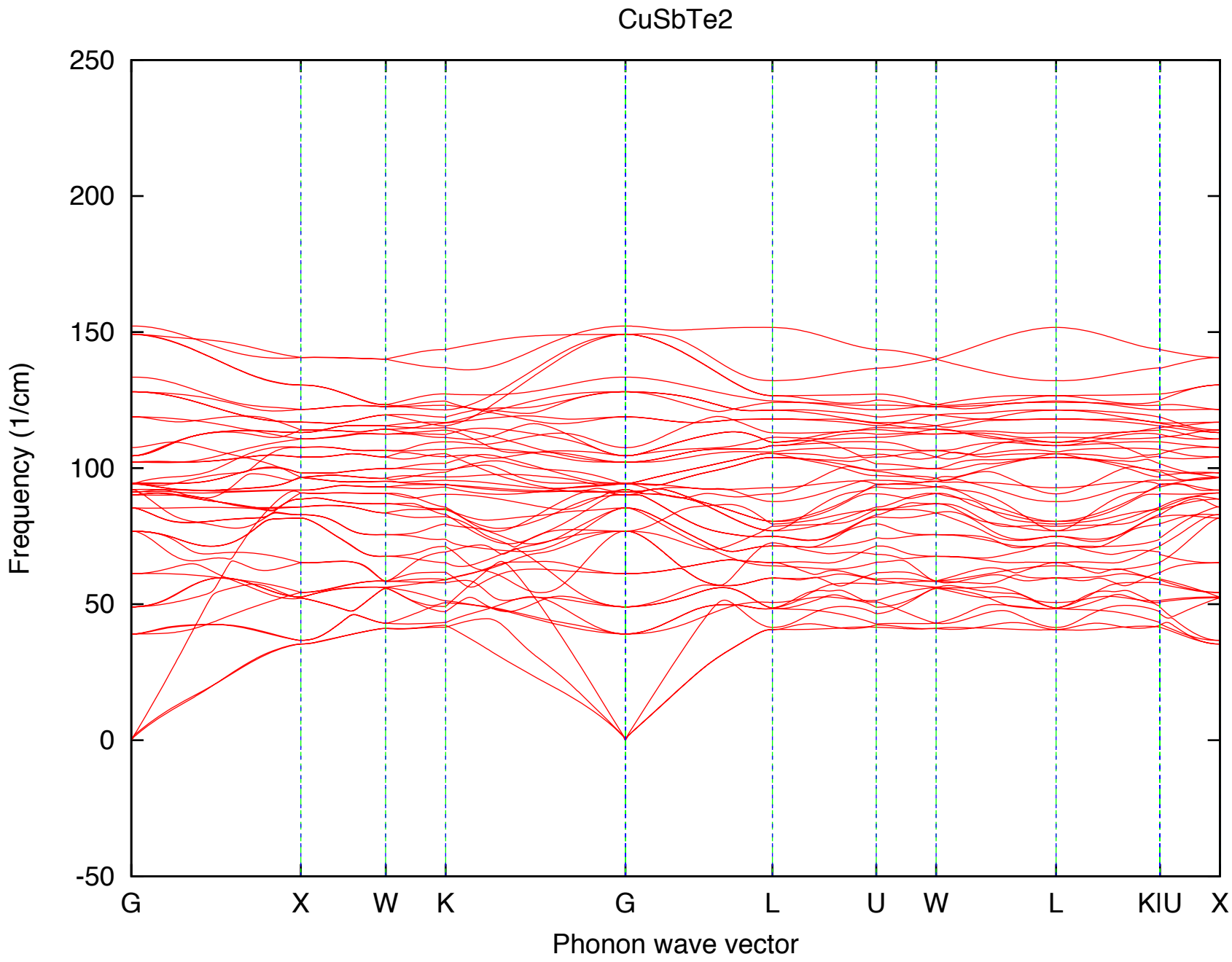

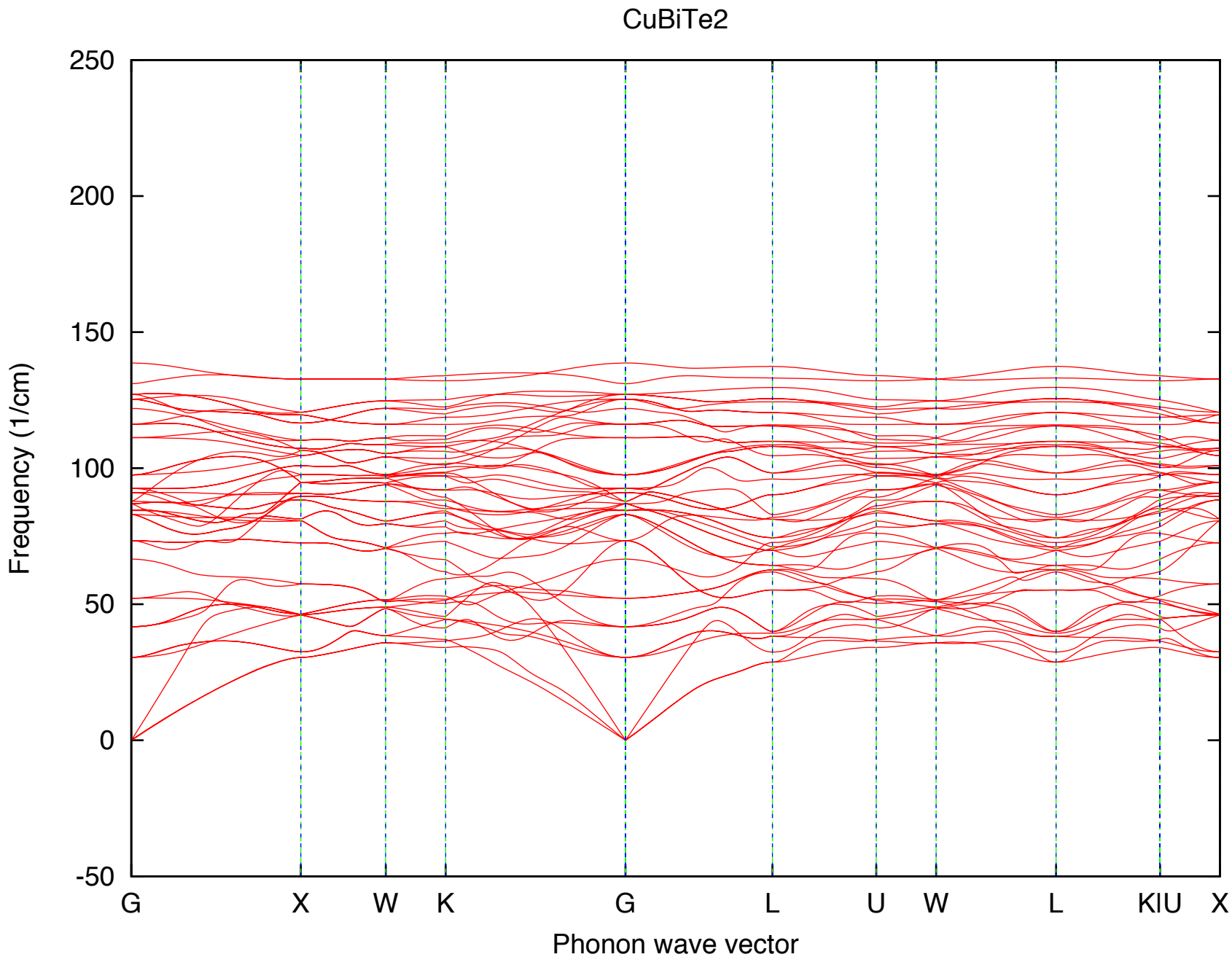
CuBiTe2
250
200
150
100
50
0
-50
Frequency (1/cm)
G
X
W
K
G
L
U
W
L
KIU
X
Phonon wave vector

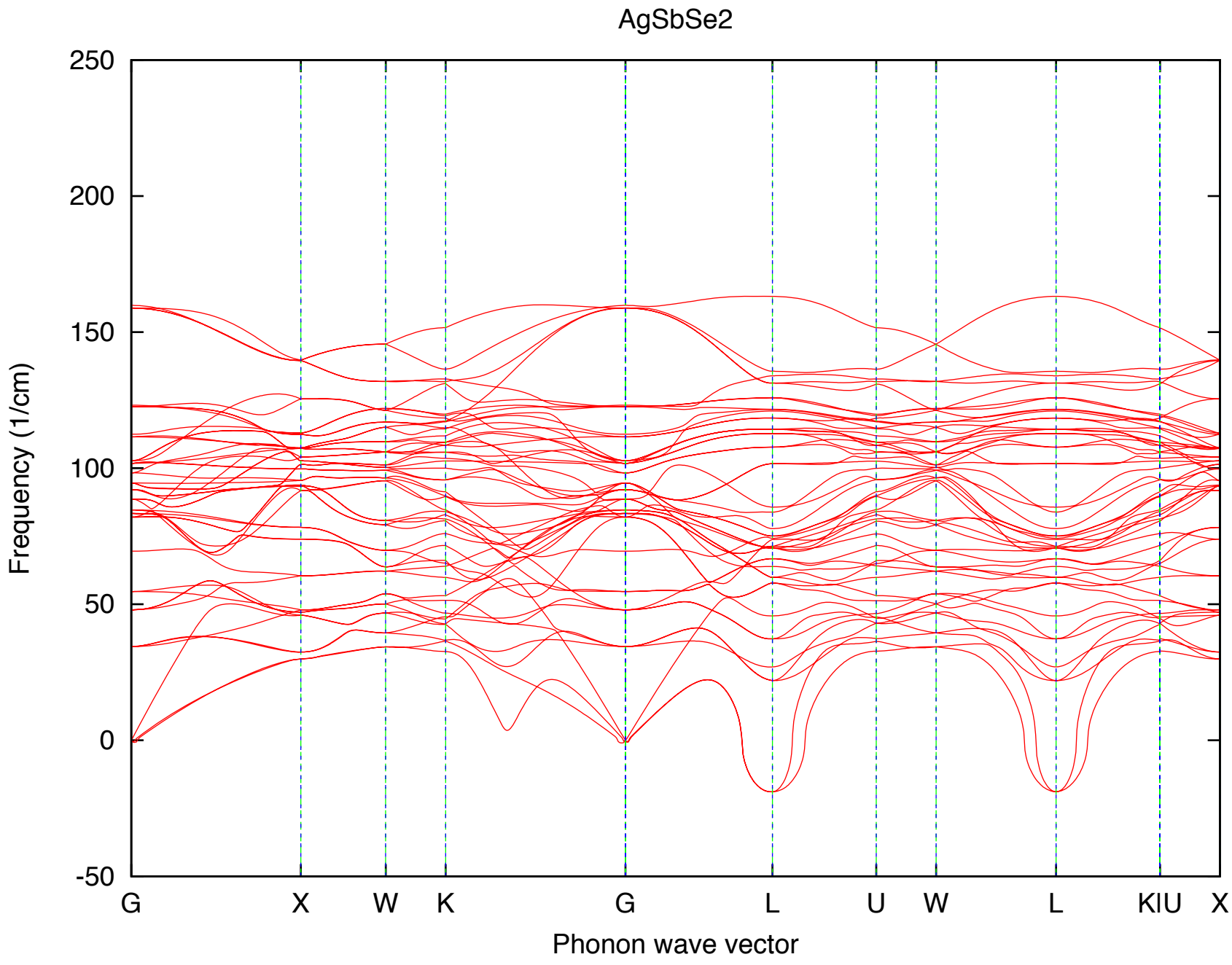
AgSbSe2
250
200
150
100
50
0
-50
Frequency (1/cm)
G
X
W
K
G
L
U
W
L
KIU
X
Phonon wave vector

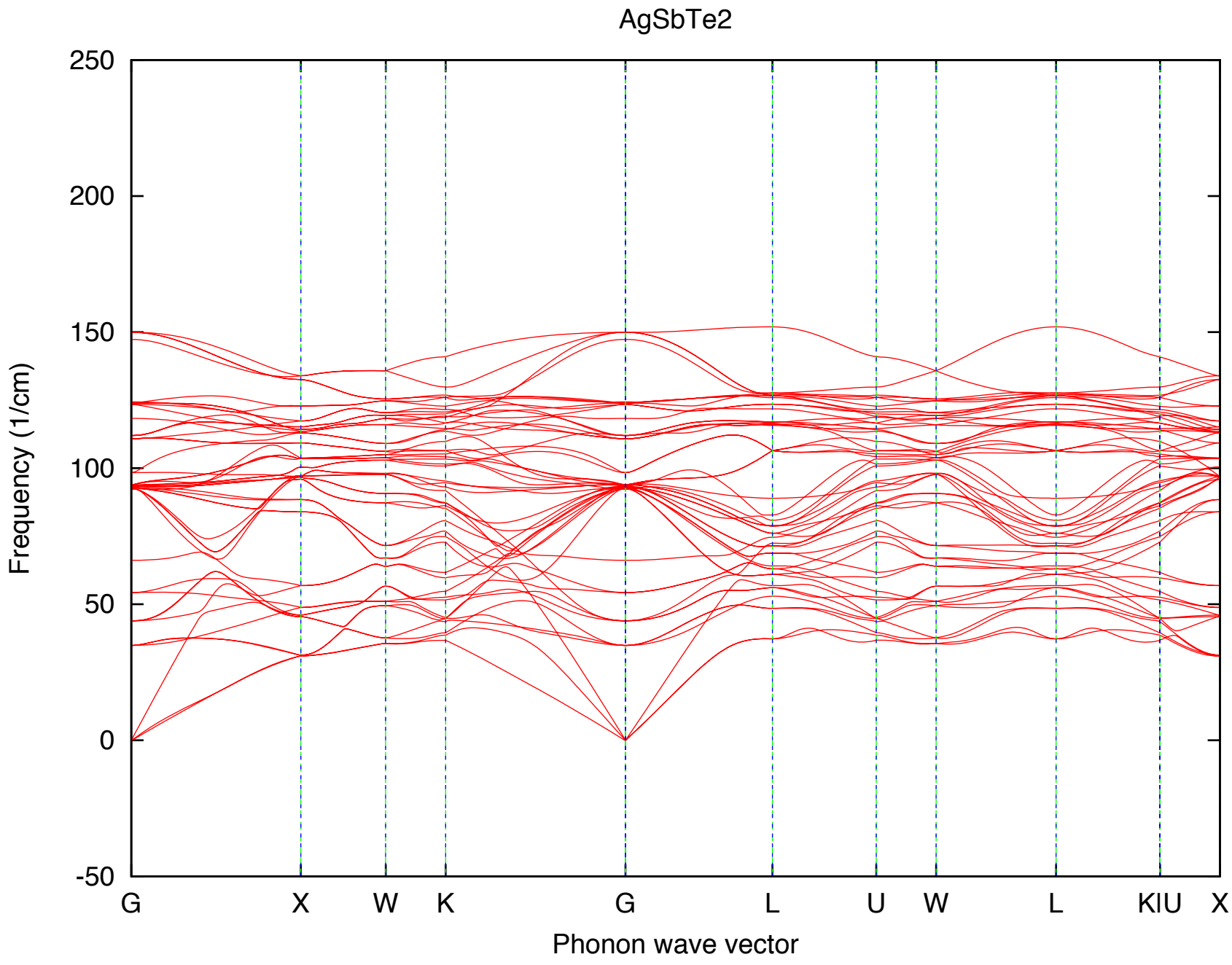

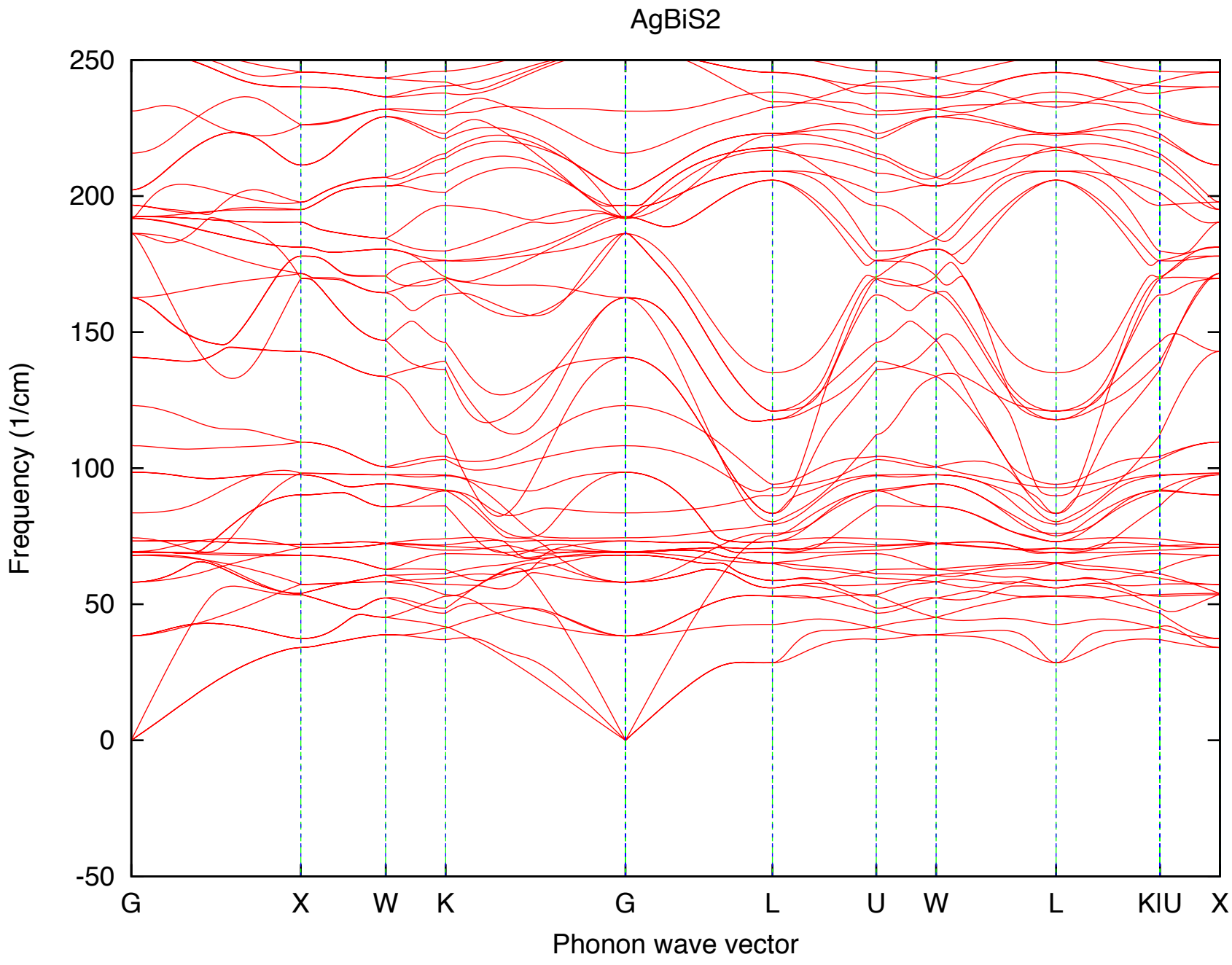

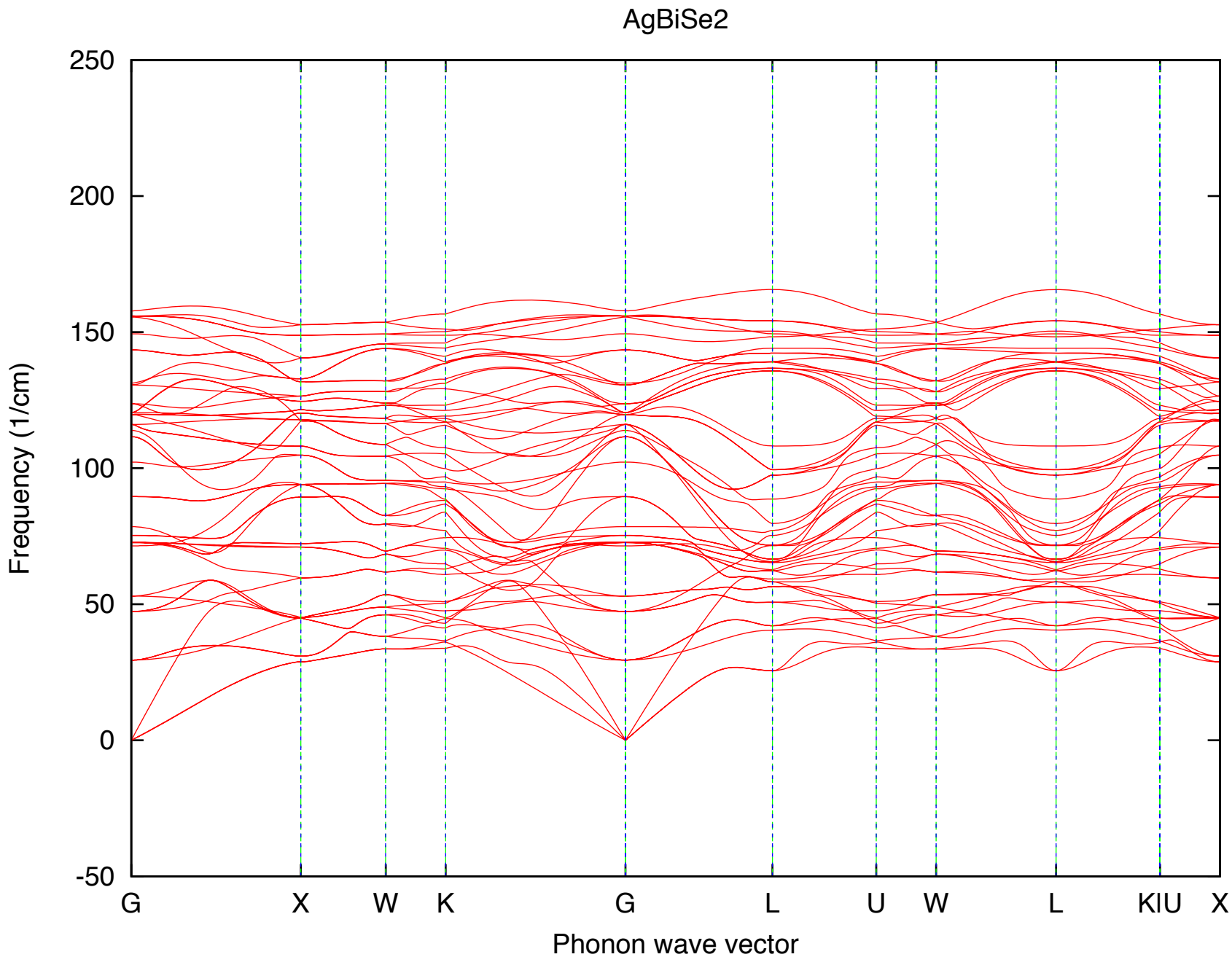

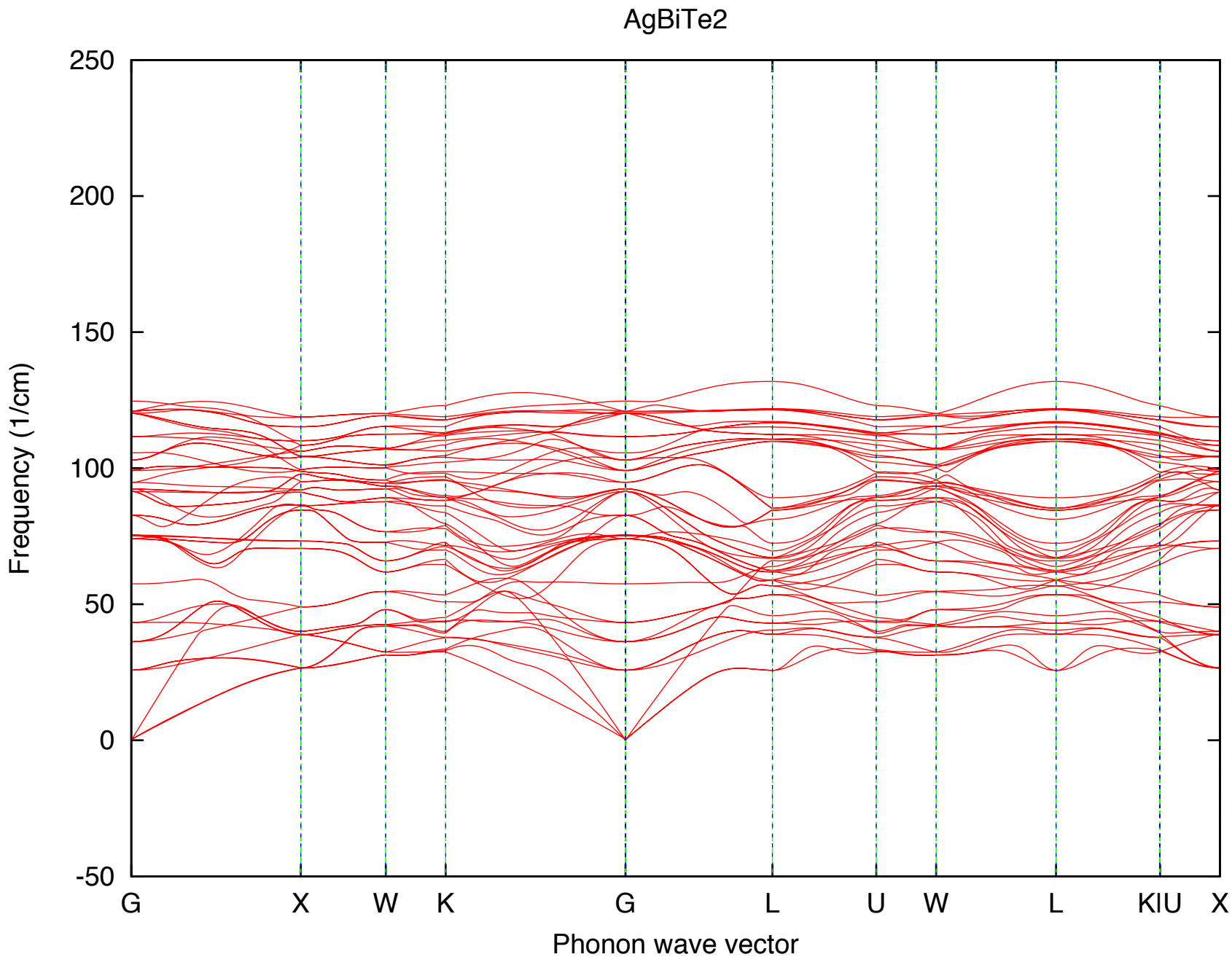
AgBiTe2
250
200
150
100
50
0
-50
Frequency (1/cm)
G
X
W
K
G
L
U
W
L
KIU
X
Phonon wave vector

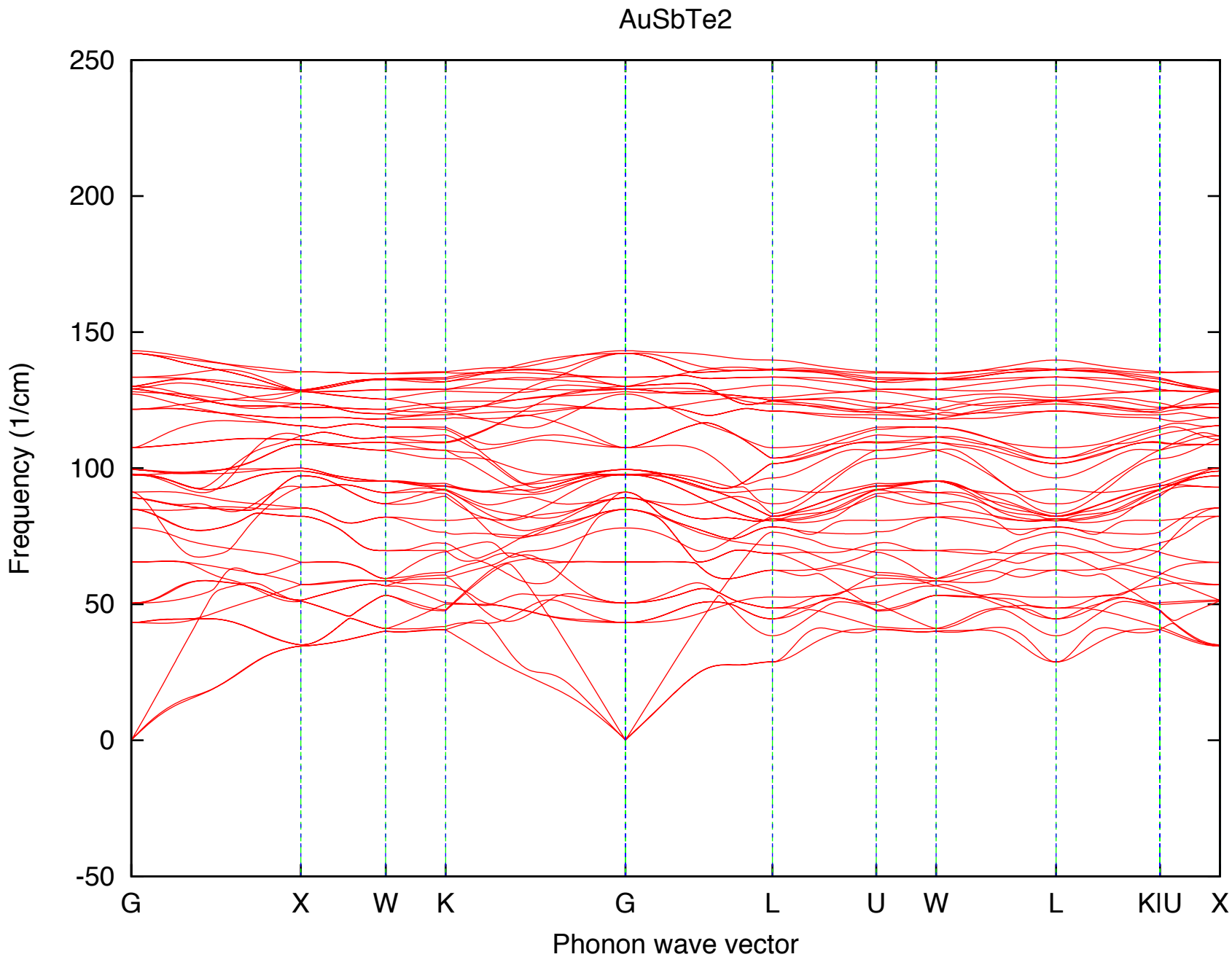

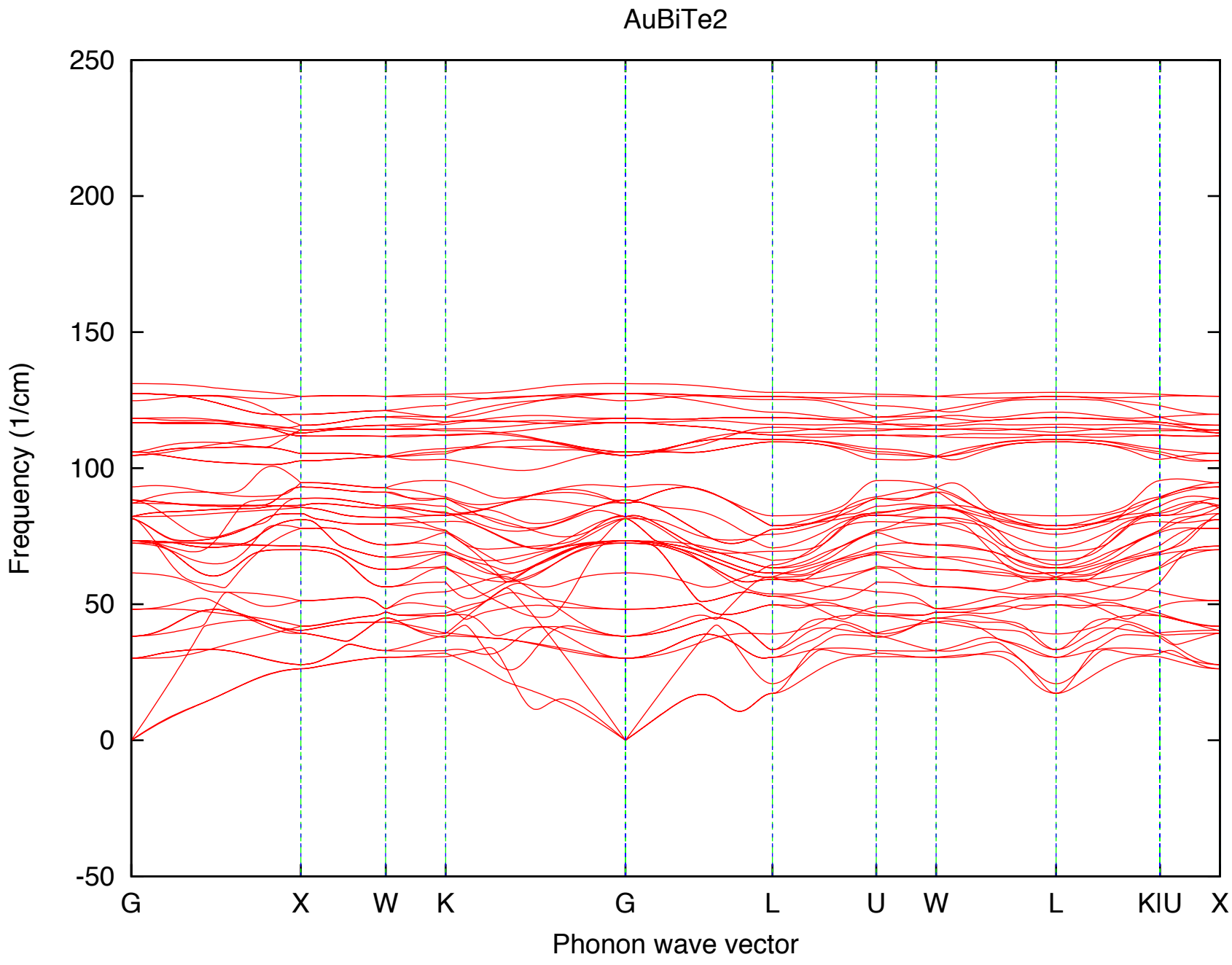
AuBiTe2
250
200
150
100
50
0
-50
Frequency (1/cm)
G
X
W
K
G
L
U
W
L
KIU
X
Phonon wave vector

6. Calculated phonon spectra of the rhombohedral rocksalt-based compounds

The Brillouin zone of the compounds with rhombohedral L11 crystal structures, the atomic arrangement shown in Fig. 1b, is shown in Fig. S7. The calculated phonon dispersions of those compounds follow, with the compound name indicated above each panel. Compounds with spectra that contain negative calculated frequencies are unstable and do not exist in the rhombohedral L11 crystal structure; accordingly, their phonons are not shown.

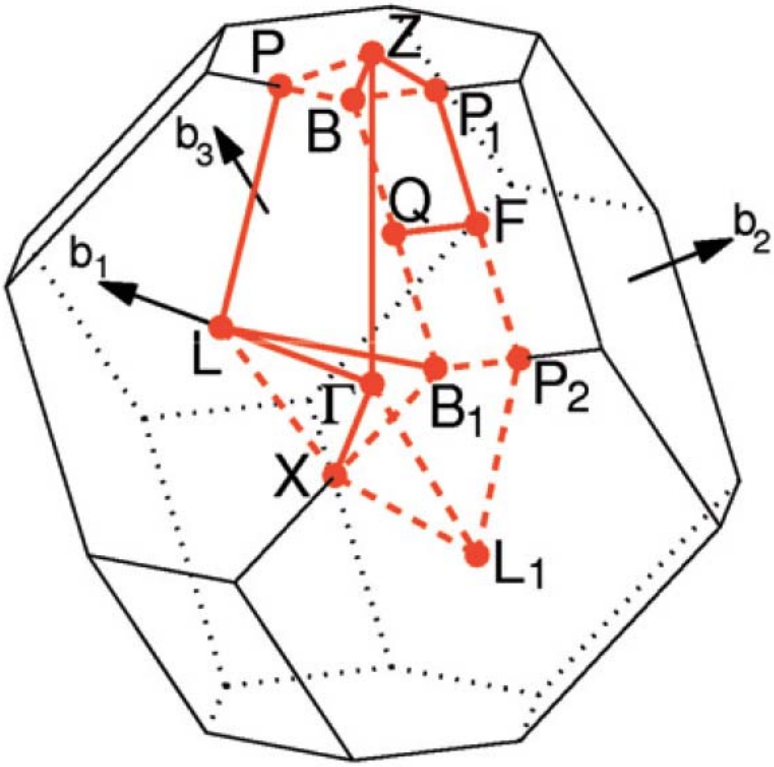

Figure S7: *Brillouin zone of rhombohedral R3m (AF-II). Phonon dispersions of the stable R3m rocksalt-based ABX_2 compounds with A=alkali metal (see below).*

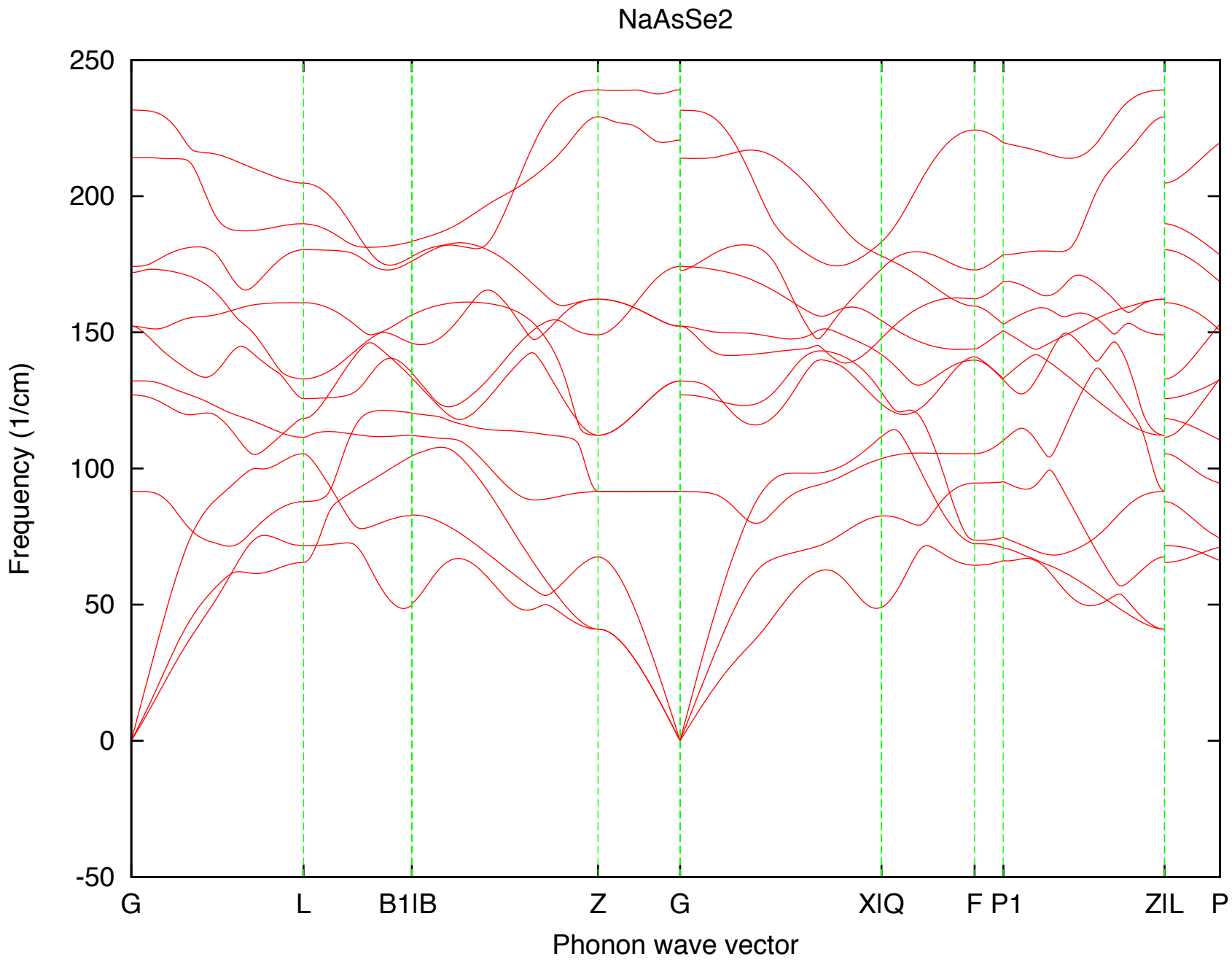
NaAsSe2
250
200
150
100
50
0
-50
Frequency (1/cm)
G
L
B1|B
Z
G
X|Q
F
P1
Z|L
P
Phonon wave vector

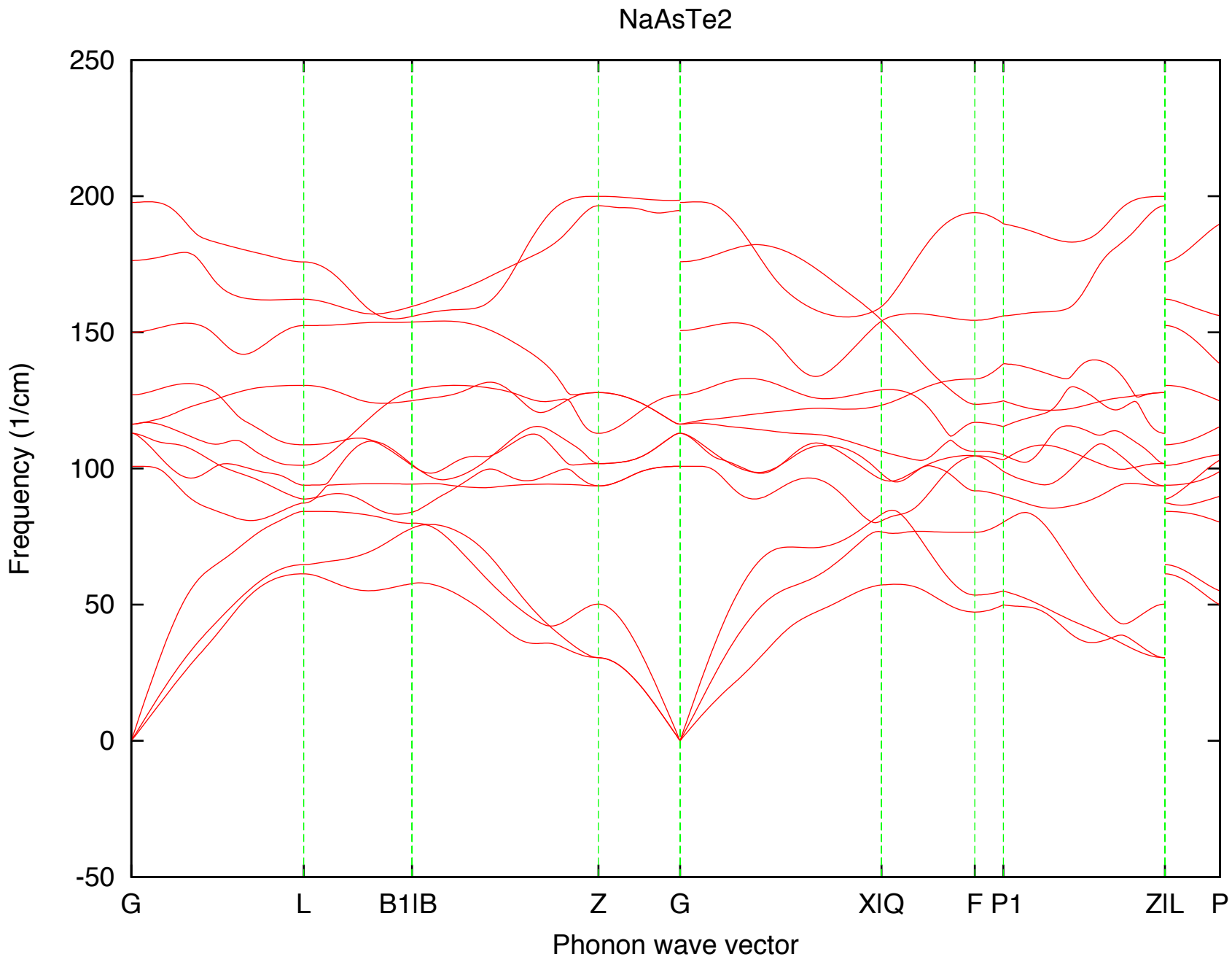
NaAsTe2
250
200
150
100
50
0
-50
Frequency (1/cm)
G
L
B1|B
Z
G
X|Q
F
P1
Z|L
P
Phonon wave vector

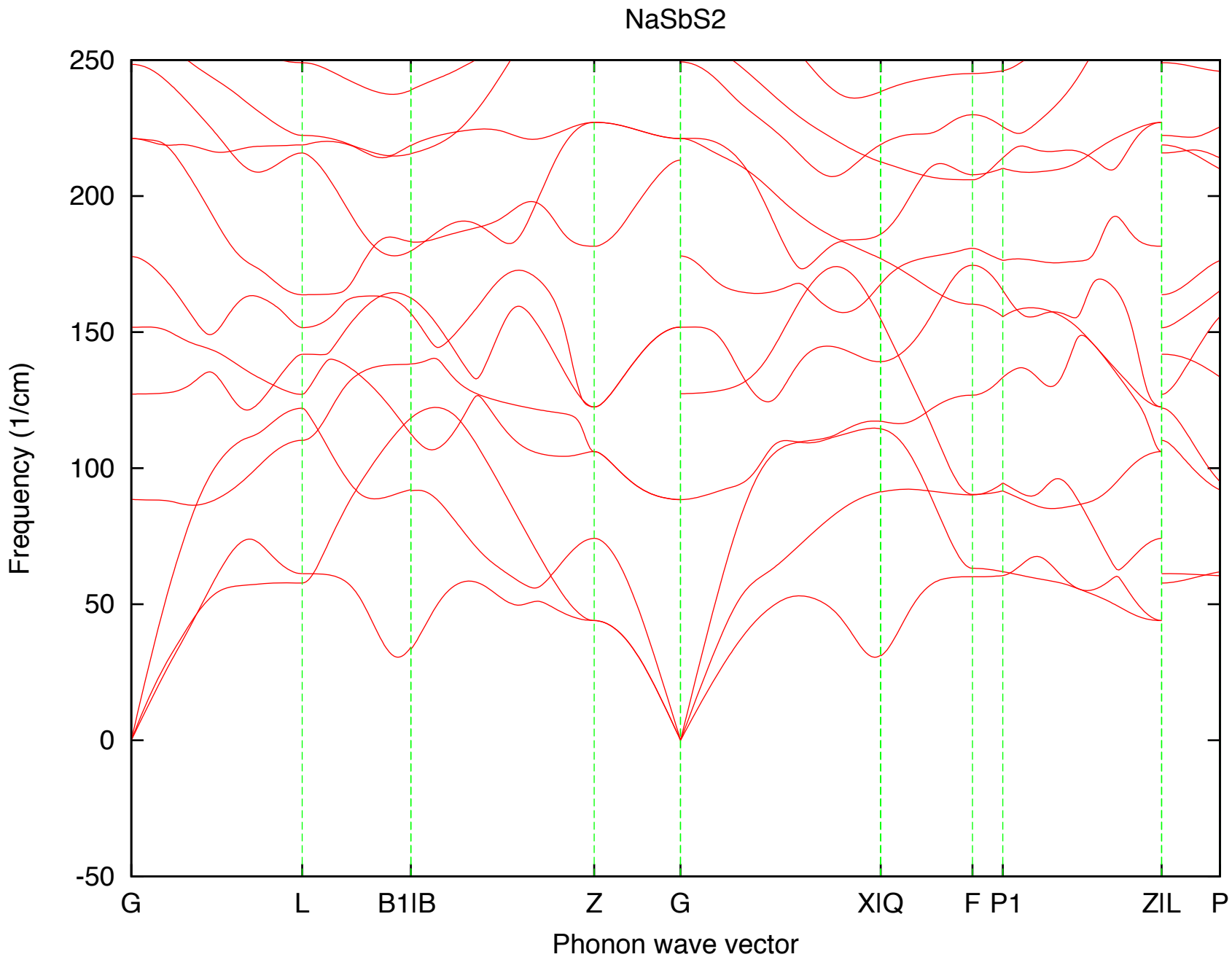
NaSbS2
250
200
150
100
50
0
-50
Frequency (1/cm)
G
L
B1|B
Z
G
X|Q
F
P1
Z|L
P
Phonon wave vector

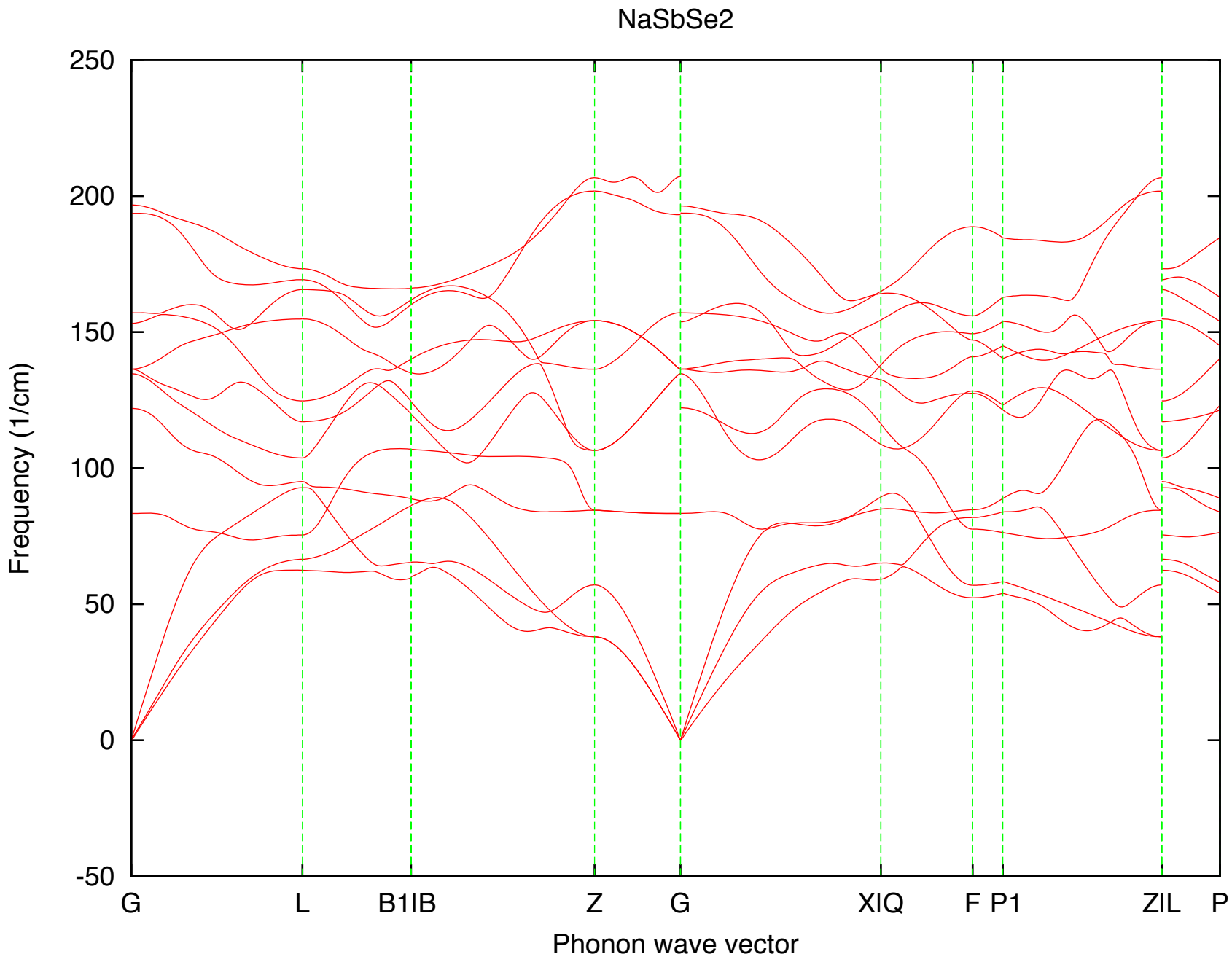

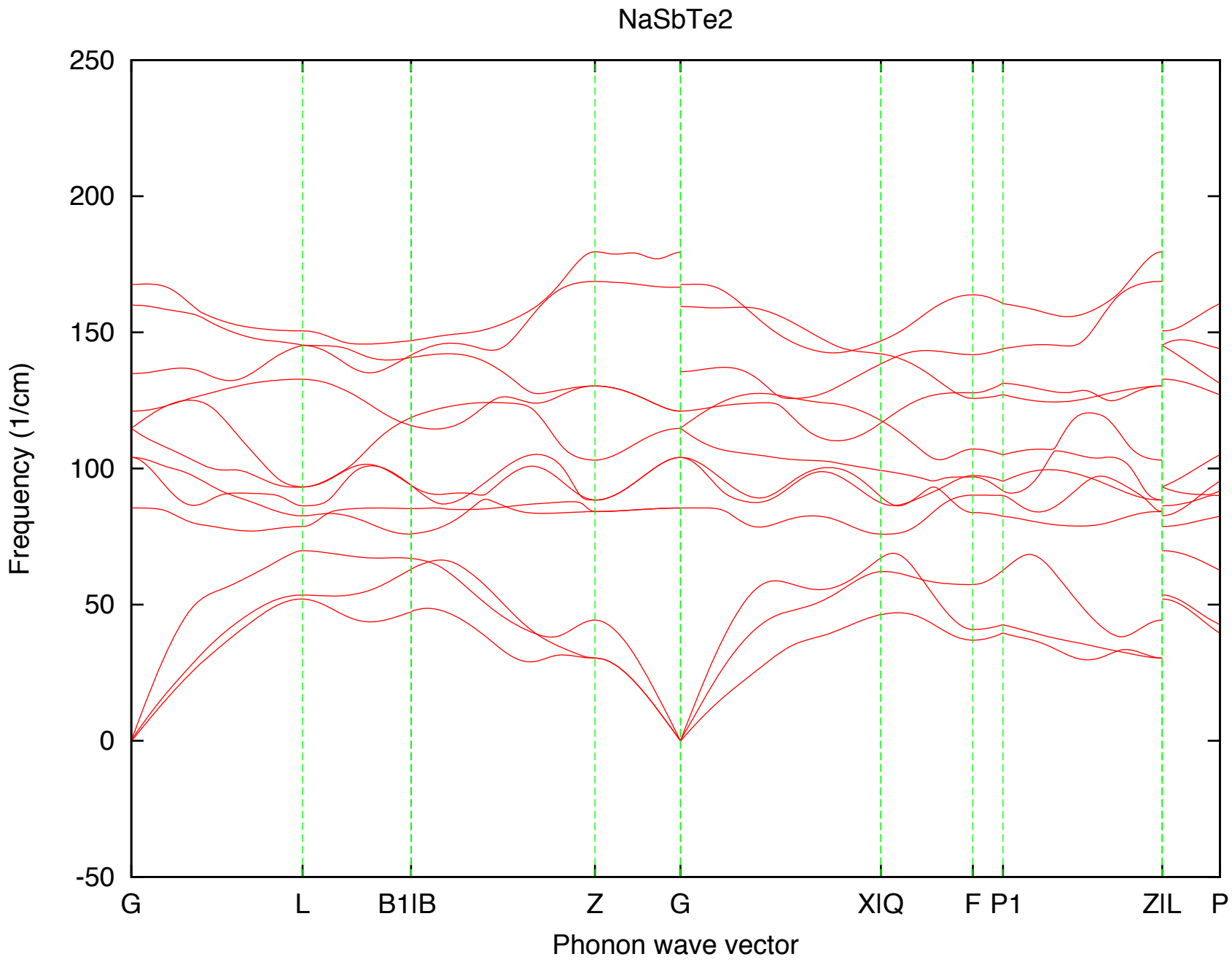
NaSbTe2
250
200
150
100
50
0
-50
Frequency (1/cm)
G
L
B1|B
Z
G
X|Q
F
P1
Z|L
P
Phonon wave vector

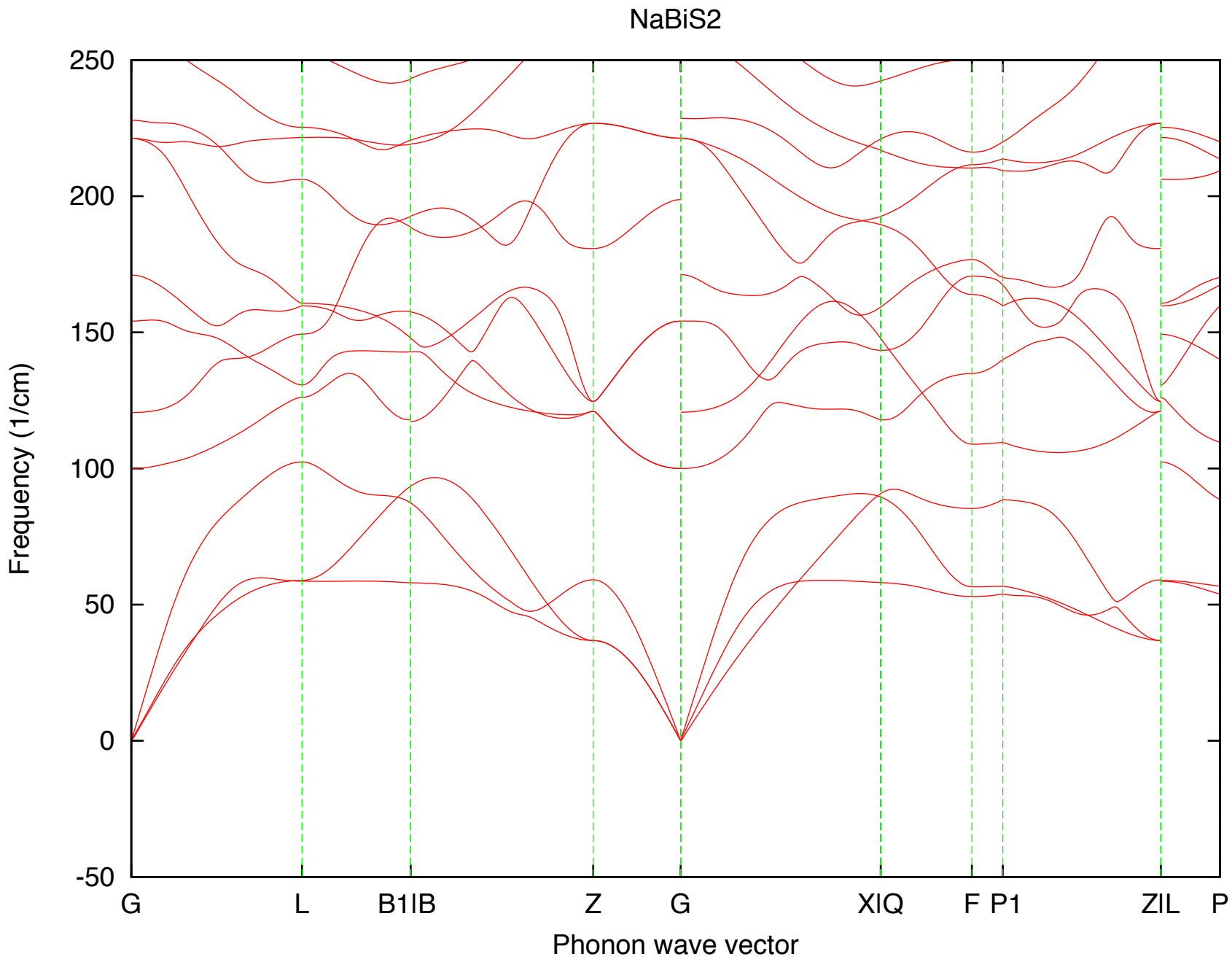
NaBiS2
250
200
150
100
50
0
-50
Frequency (1/cm)
G
L
B1|B
Z
G
X|Q
F
P1
Z|L
P
Phonon wave vector

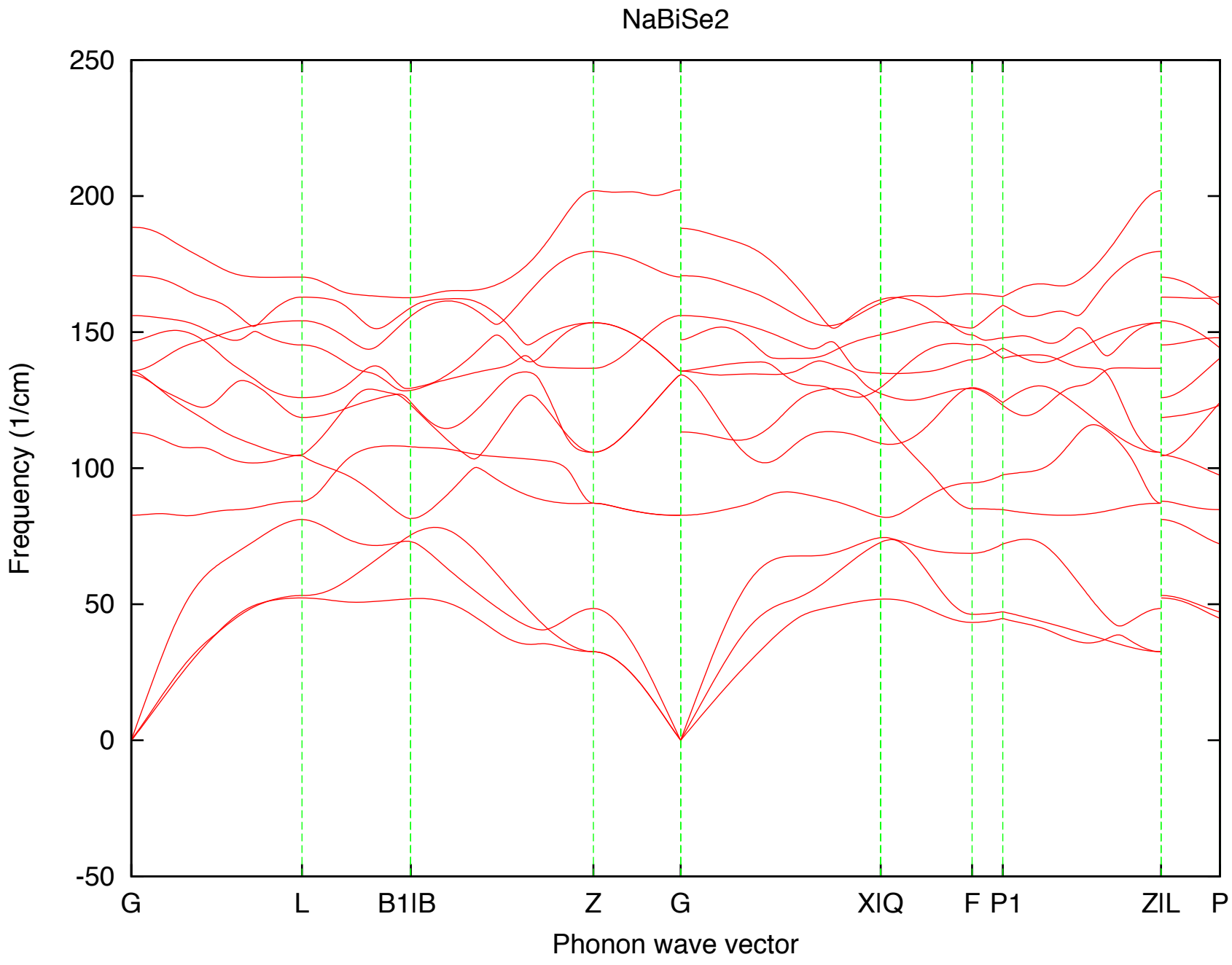
NaBiSe2
250
200
150
100
50
0
-50
Frequency (1/cm)
G
L
B1|B
Z
G
X|Q
F
P1
Z|L
P
Phonon wave vector

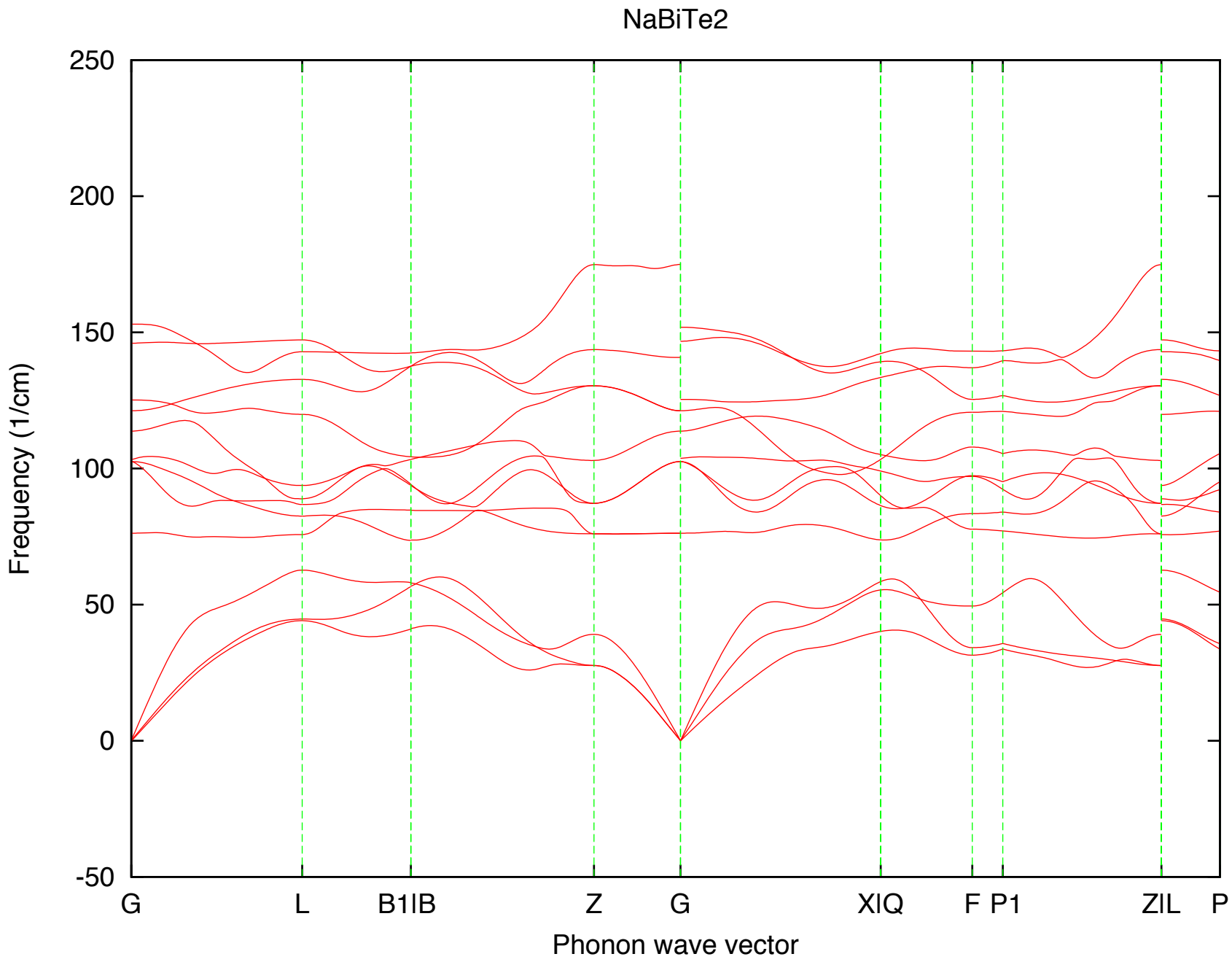
NaBiTe2
250
200
150
100
50
0
-50
Frequency (1/cm)
G
L
B1|B
Z
G
X|Q
F
P1
Z|L
P
Phonon wave vector

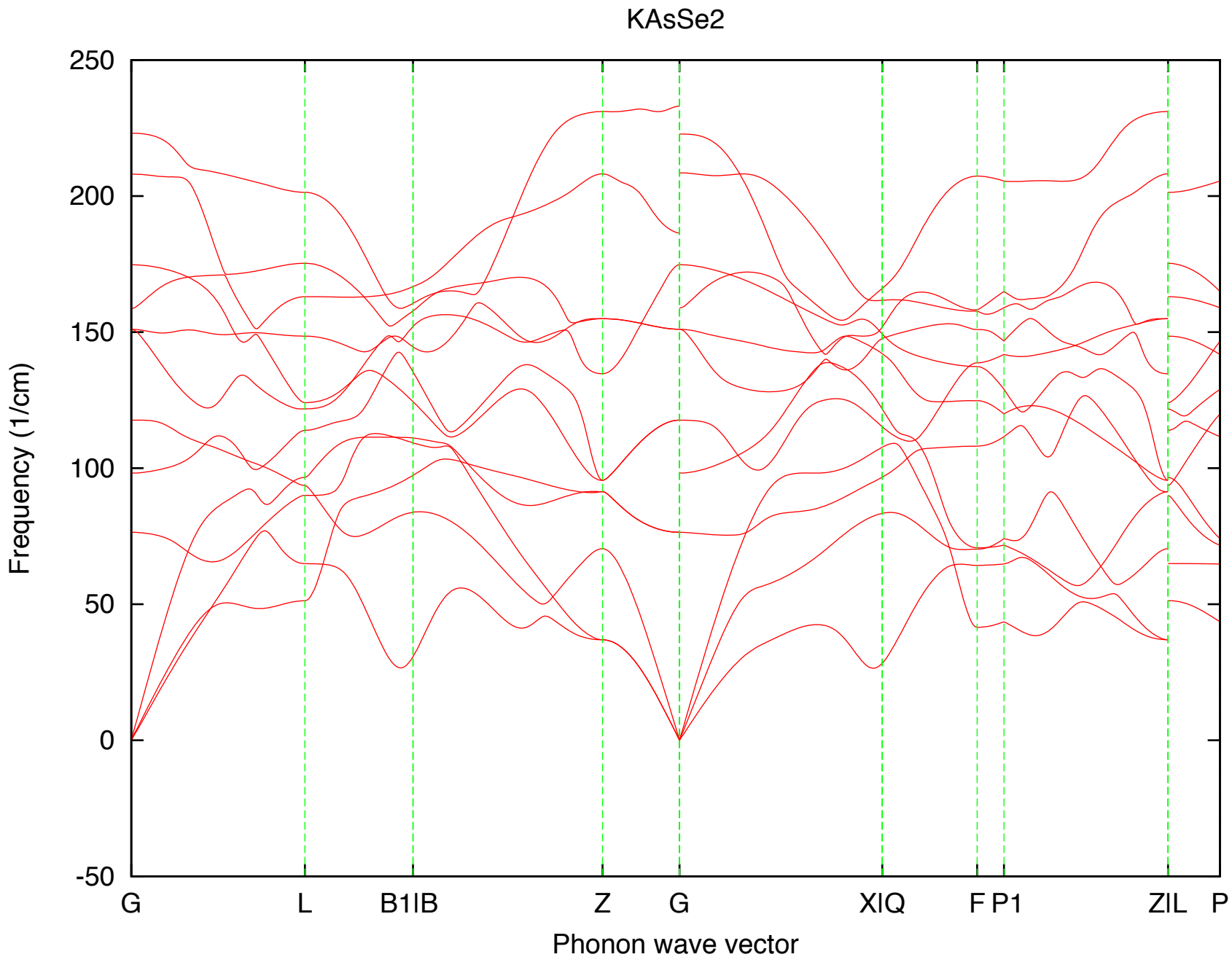

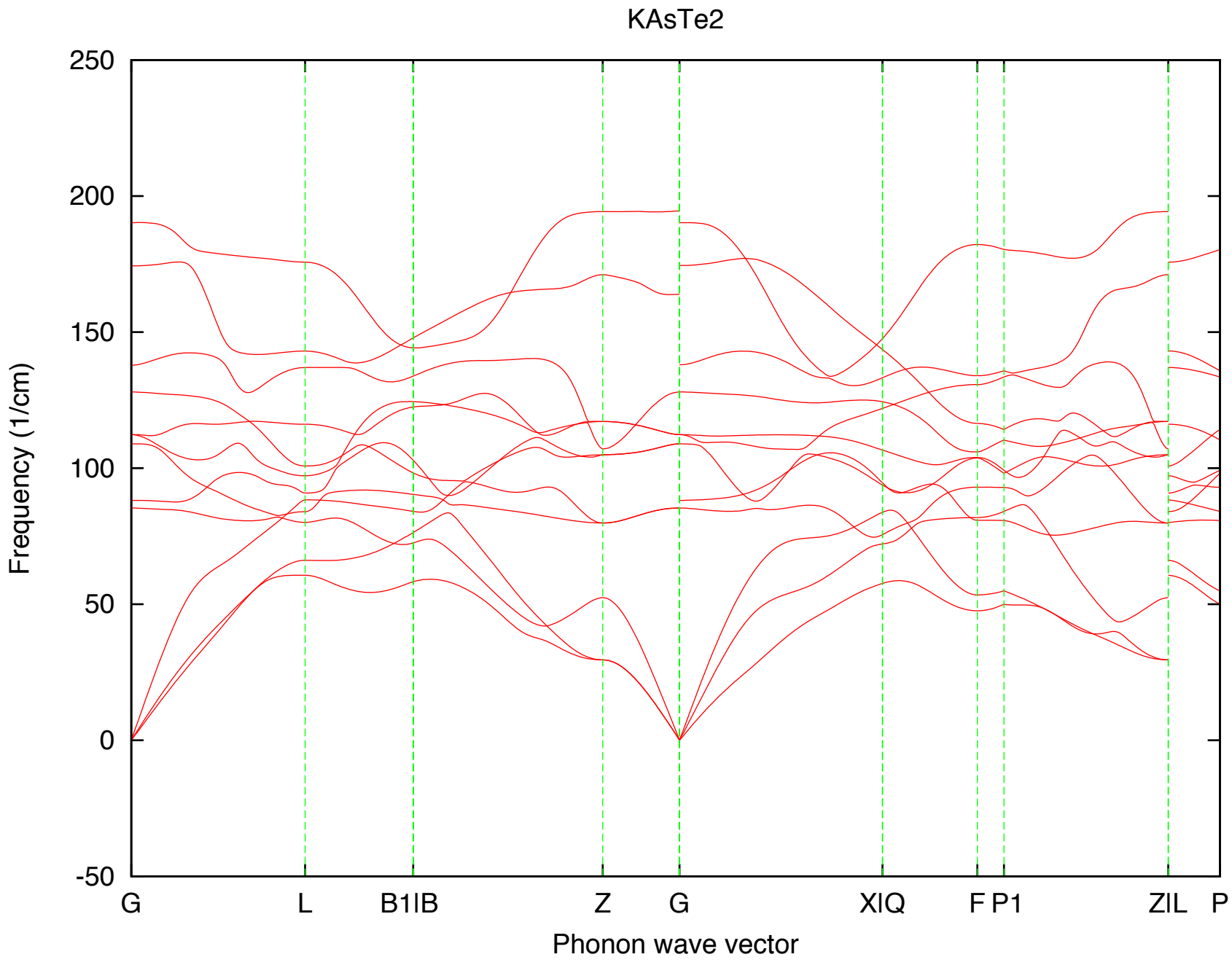
KAsTe2
250
200
150
100
50
0
-50
Frequency (1/cm)
G
L
B1|B
Z
G
X|Q
F
P1
Z|L
P
Phonon wave vector

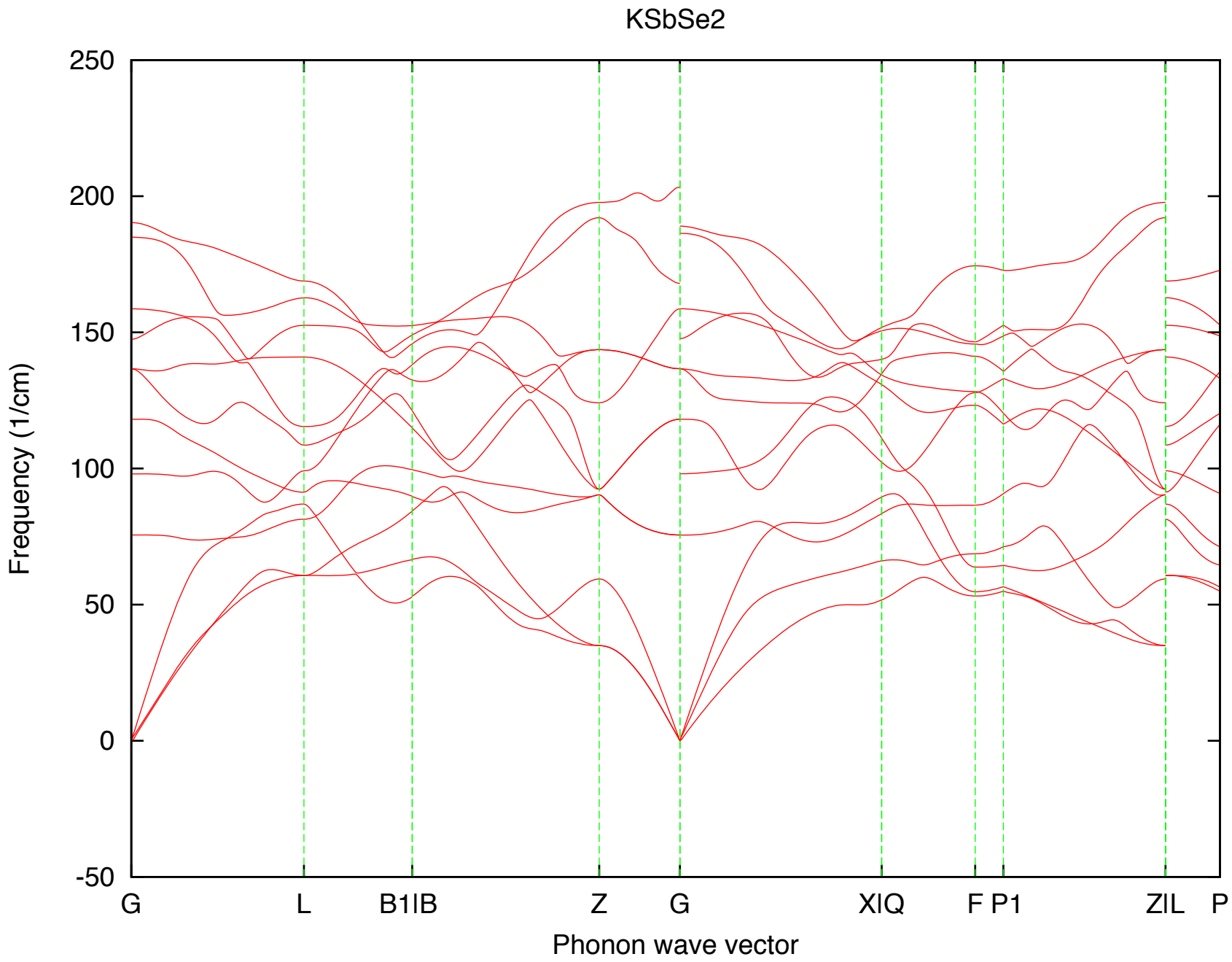
KSbSe2
250
200
150
100
50
0
-50
Frequency (1/cm)
G
L
B1|B
Z
G
X|Q
F
P1
Z|L
P
Phonon wave vector

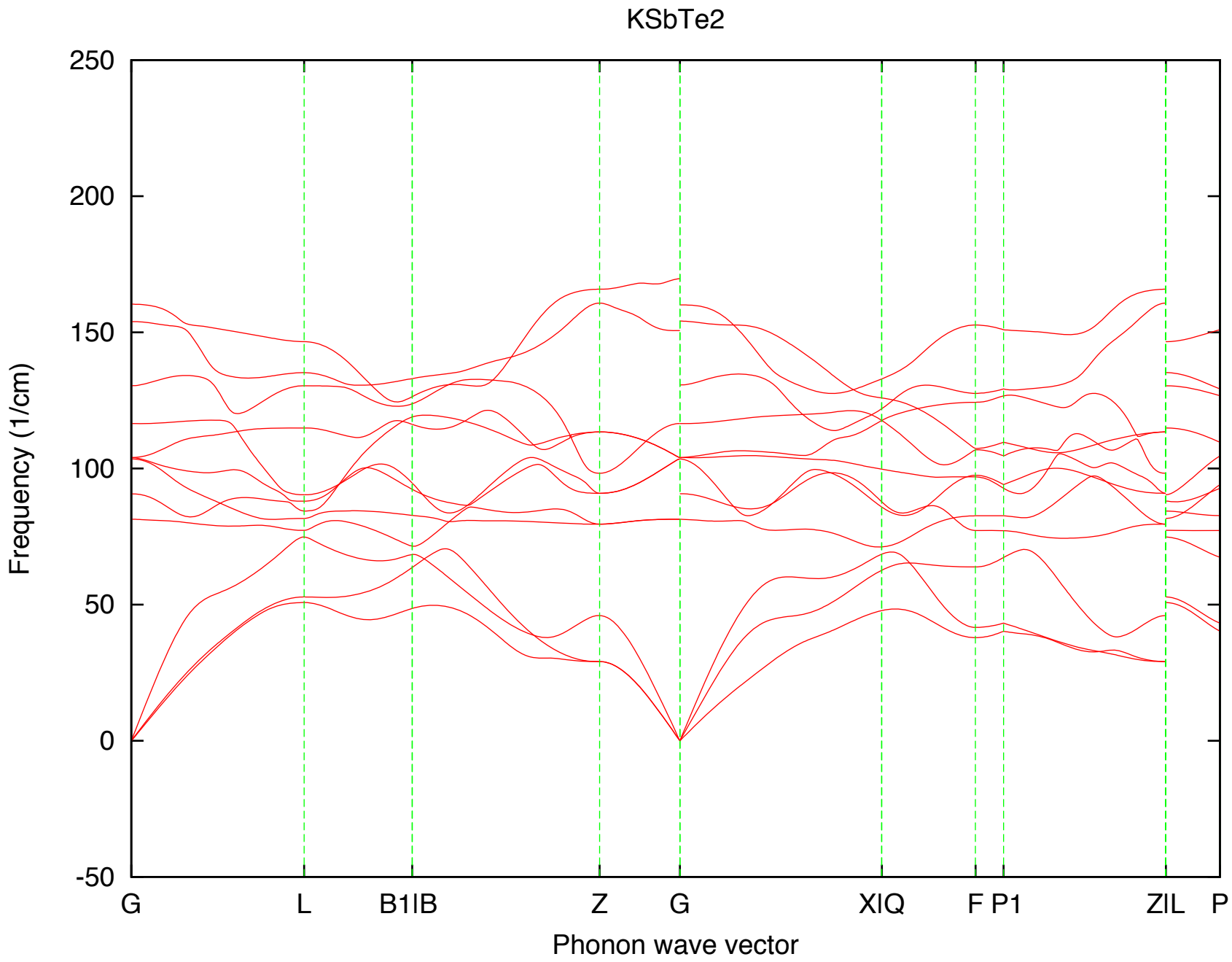
KSbTe2
250
200
150
100
50
0
-50
Frequency (1/cm)
G
L
B1|B
Z
G
X|Q
F
P1
Z|L
P
Phonon wave vector

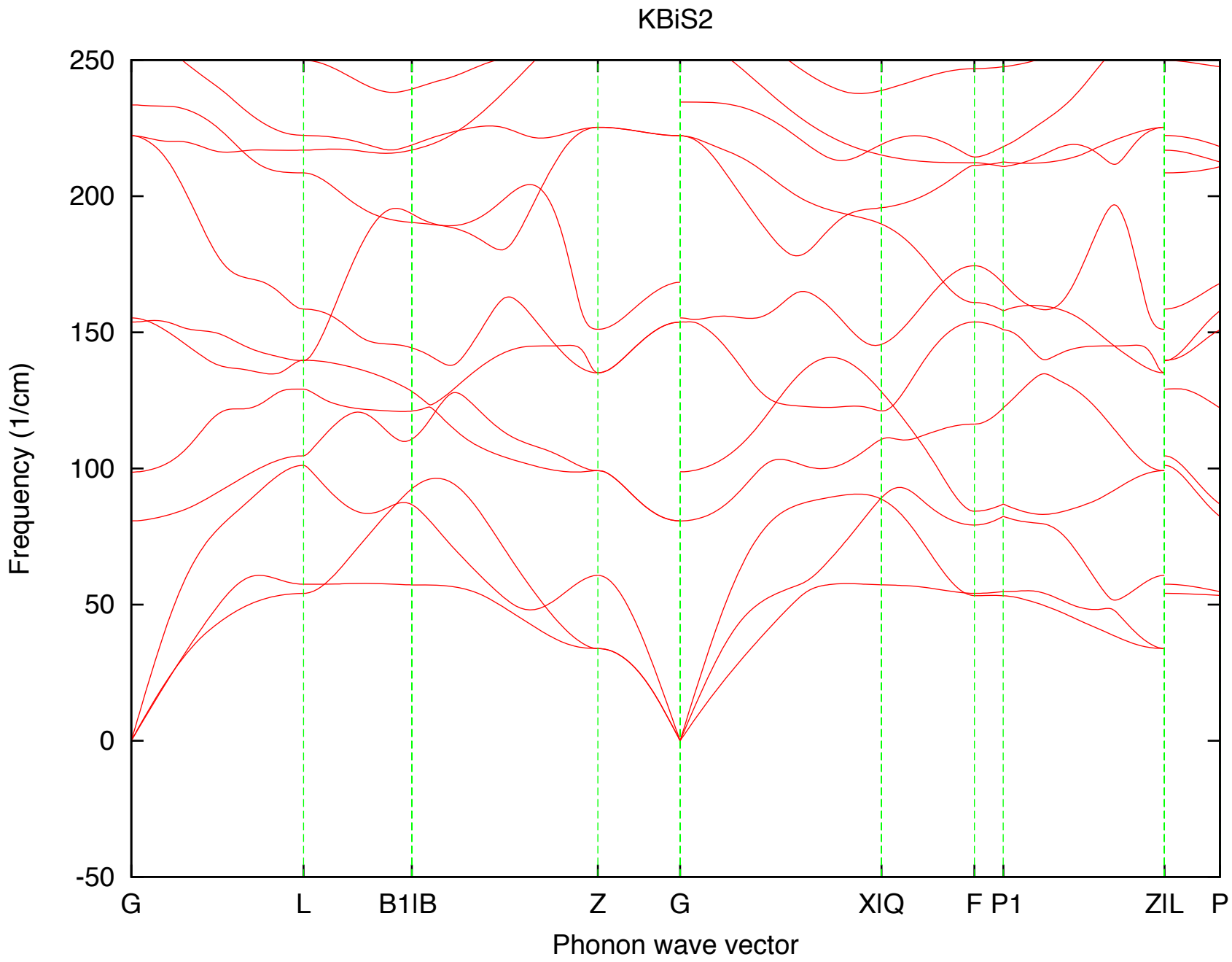
KBiS2
250
200
150
100
50
0
-50
Frequency (1/cm)
G
L
B1|B
Z
G
X|Q
F
P1
Z|L
P
Phonon wave vector

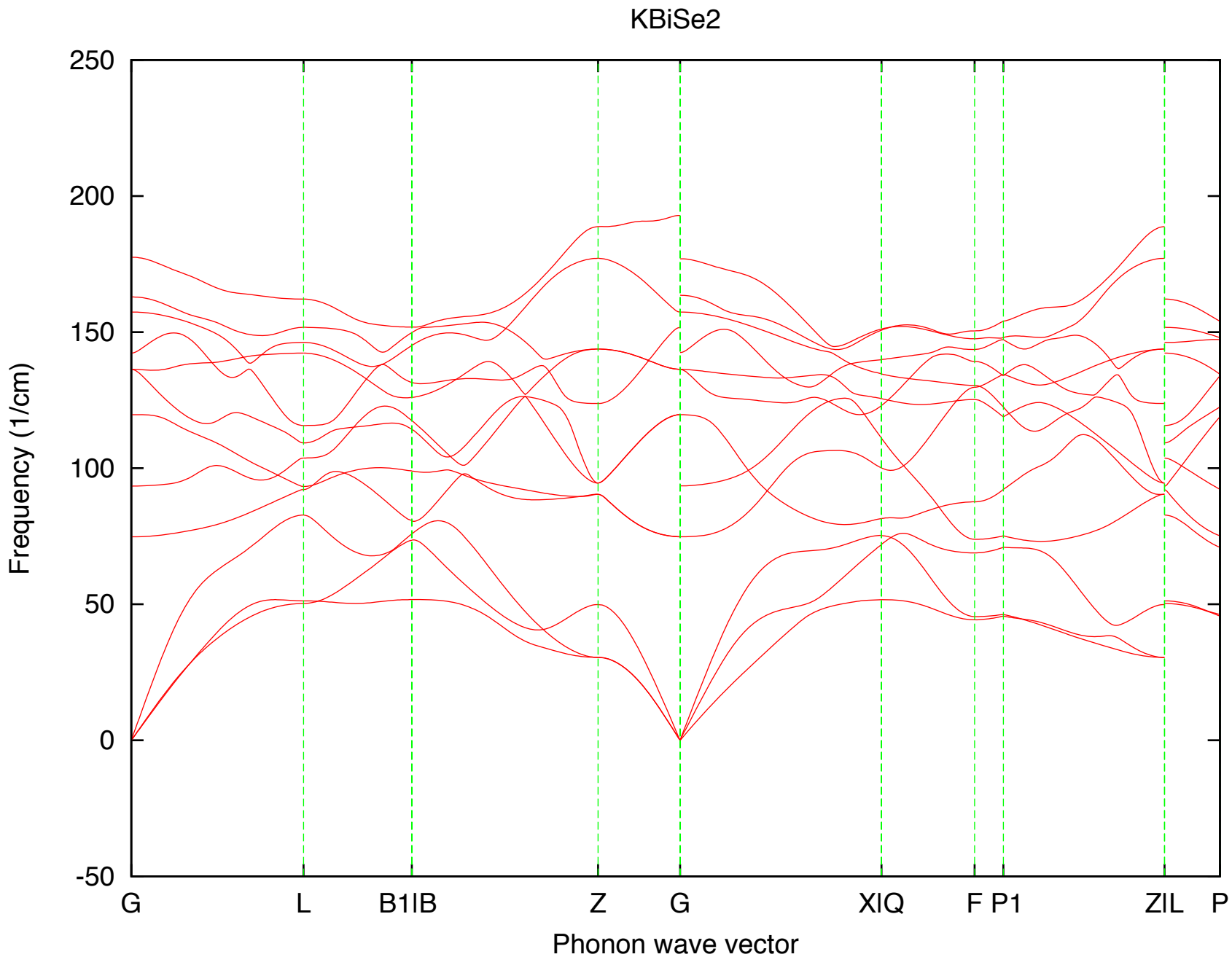

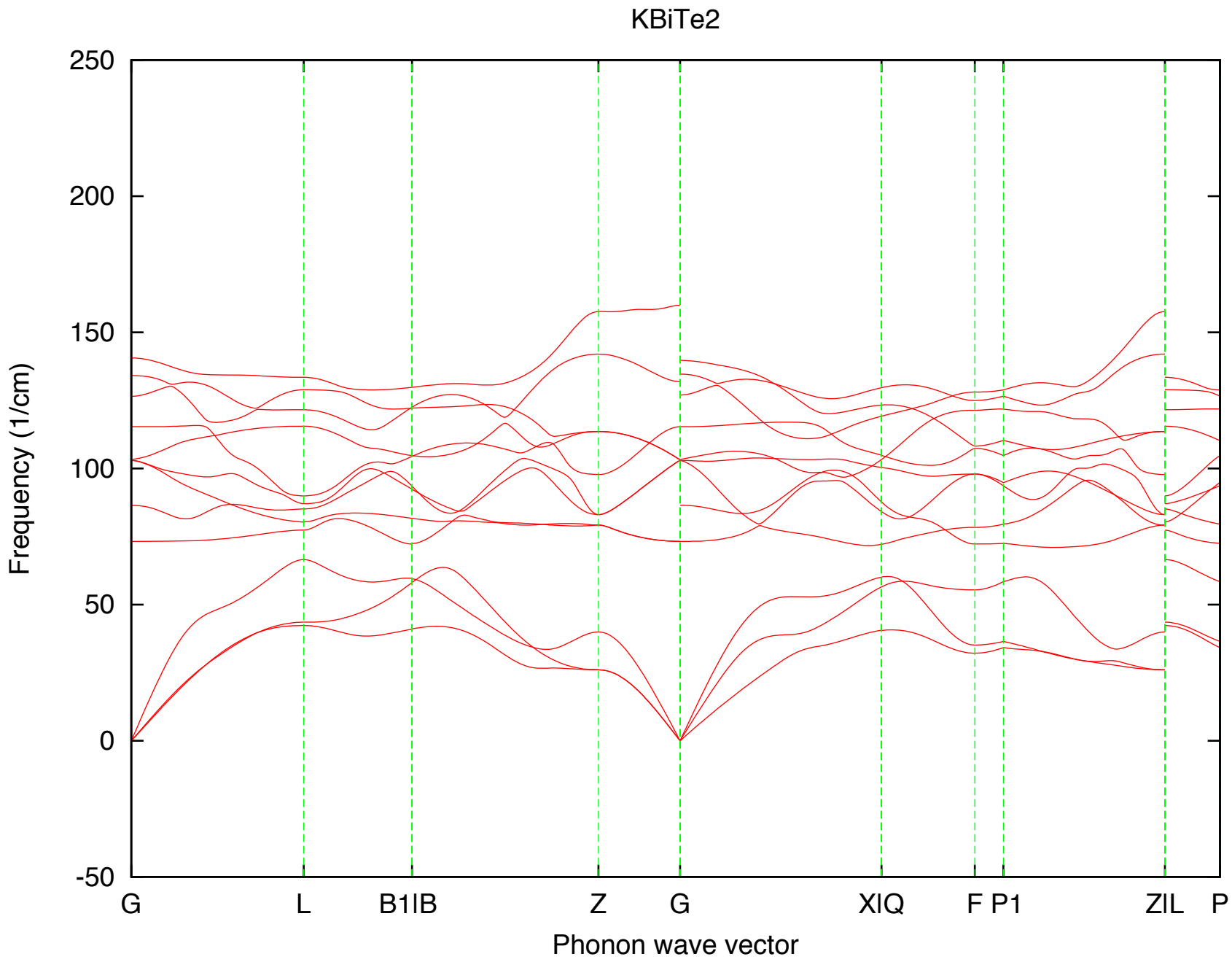

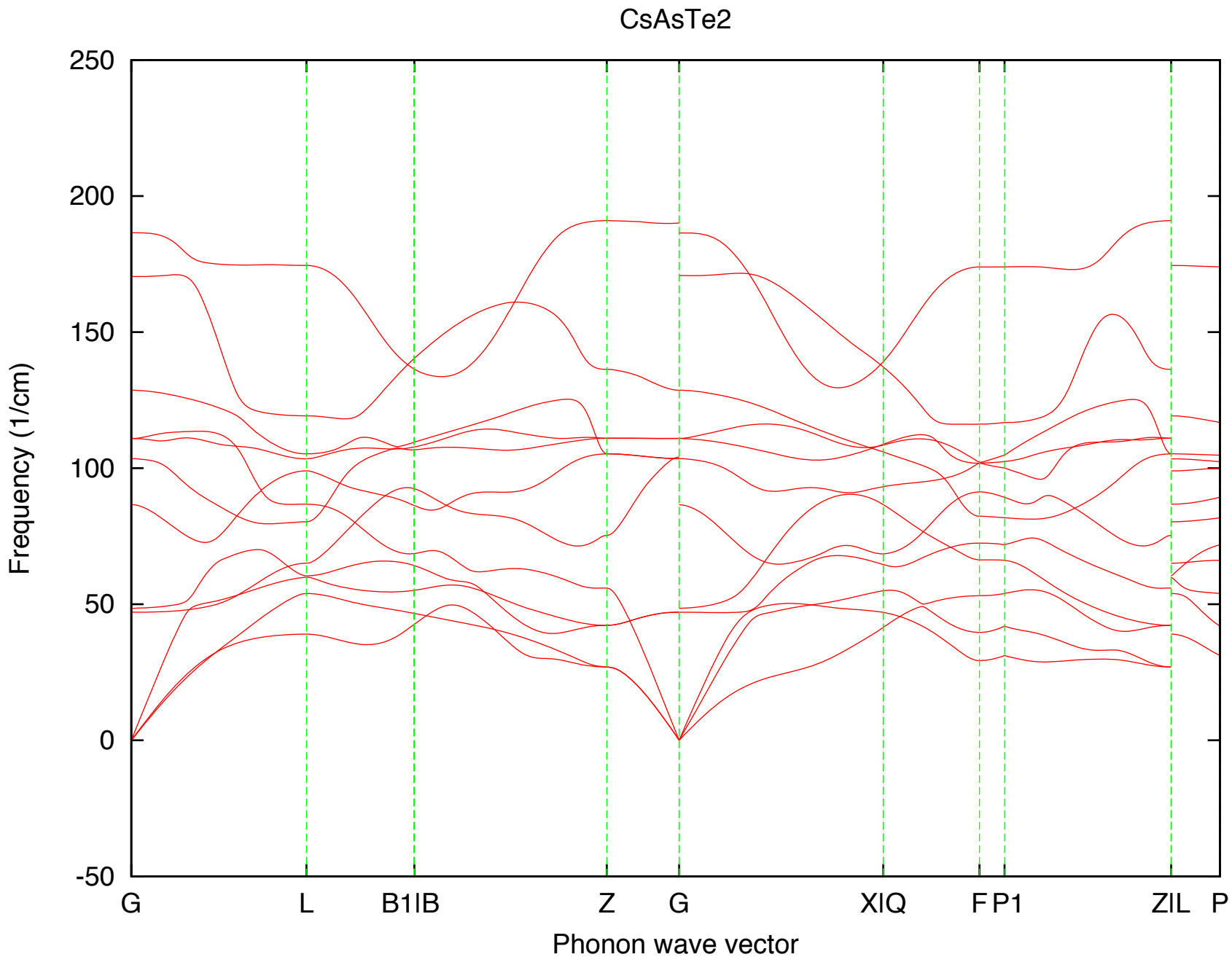

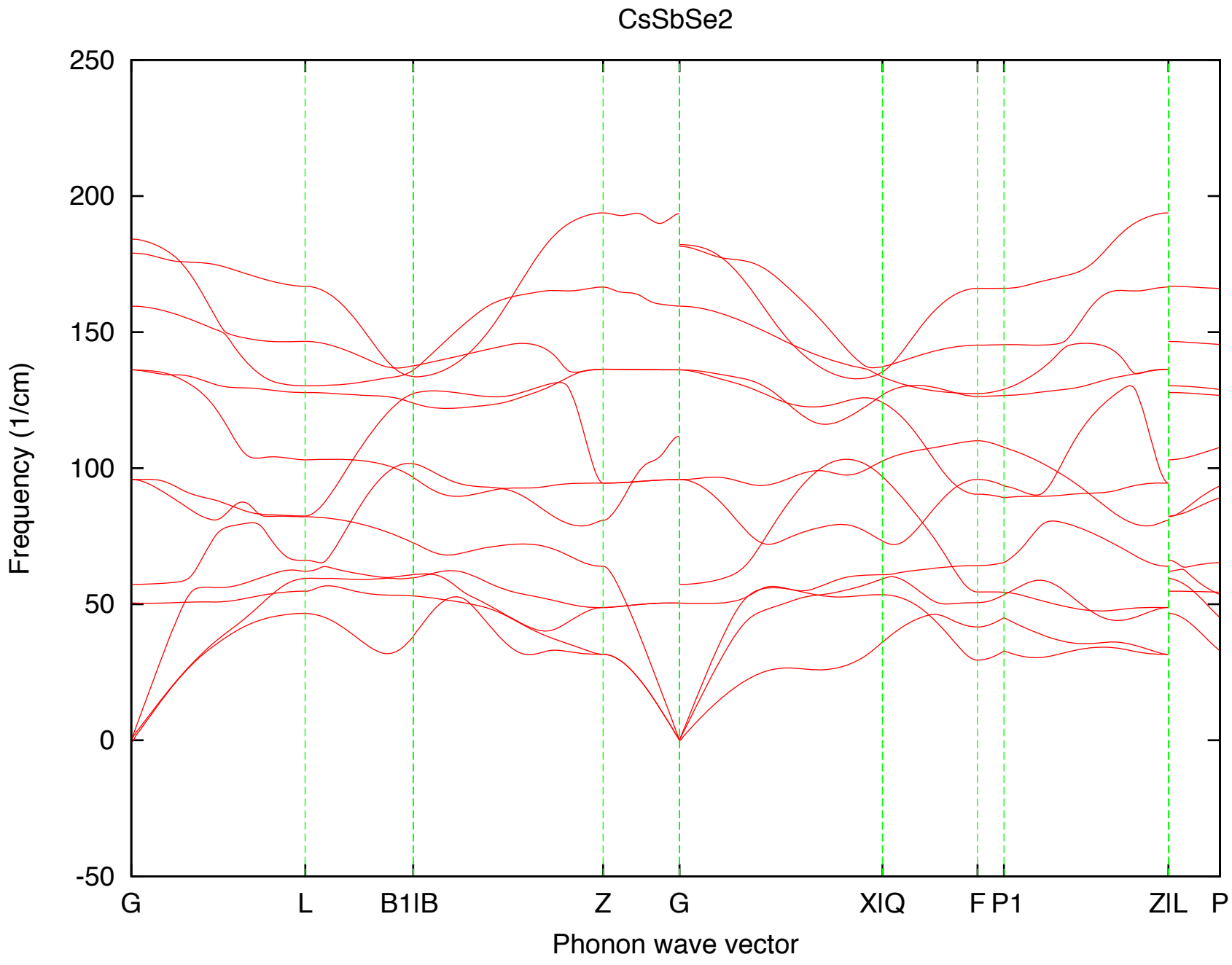
CsSbSe2
250
200
150
100
50
0
-50
Frequency (1/cm)
G
L
B1|B
Z
G
X|Q
F P1
Z|L
P
Phonon wave vector

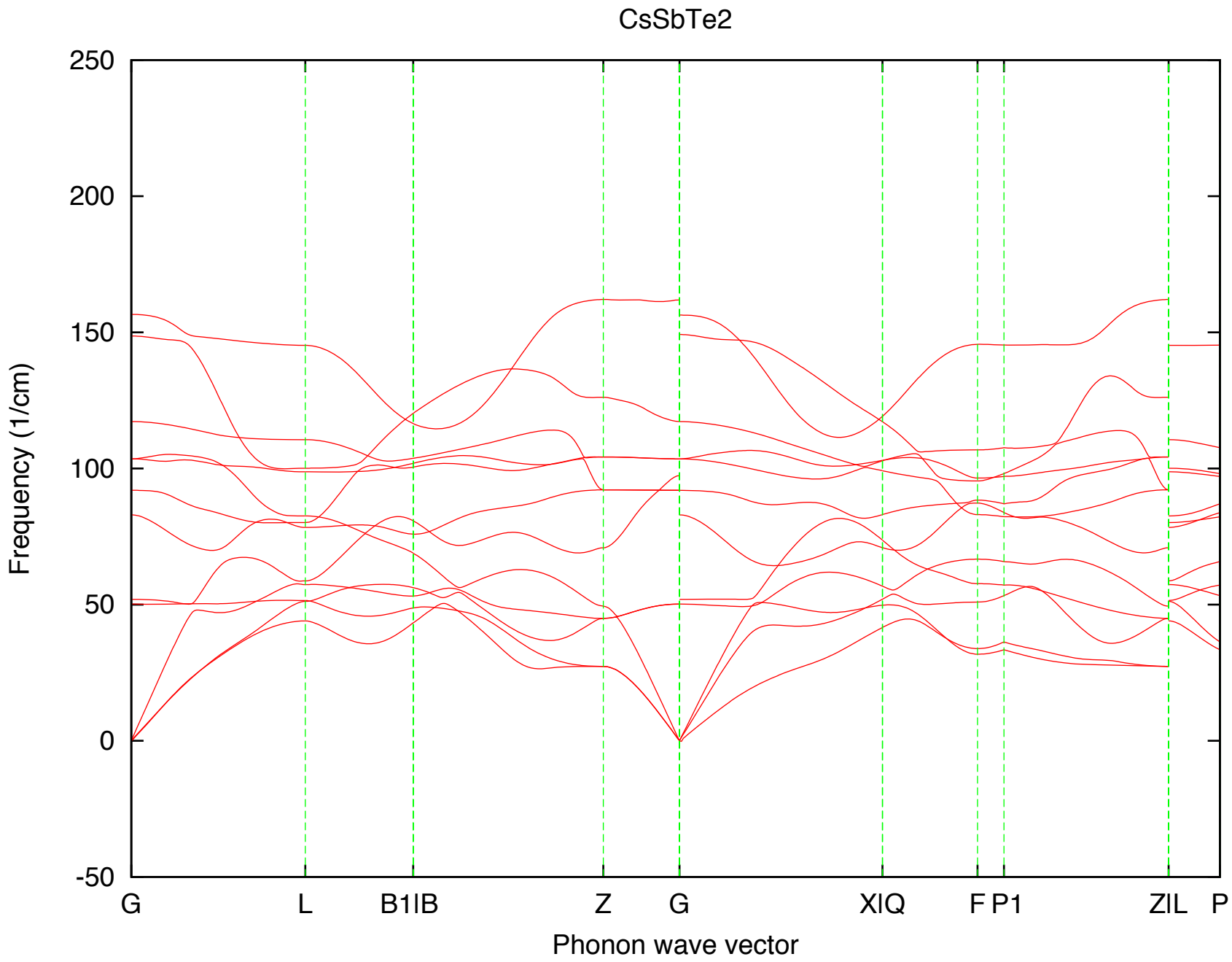
CsSbTe2
250
200
150
100
50
0
-50
Frequency (1/cm)
G
L
B1|B
Z
G
X|Q
F P1
Z|L
P
Phonon wave vector

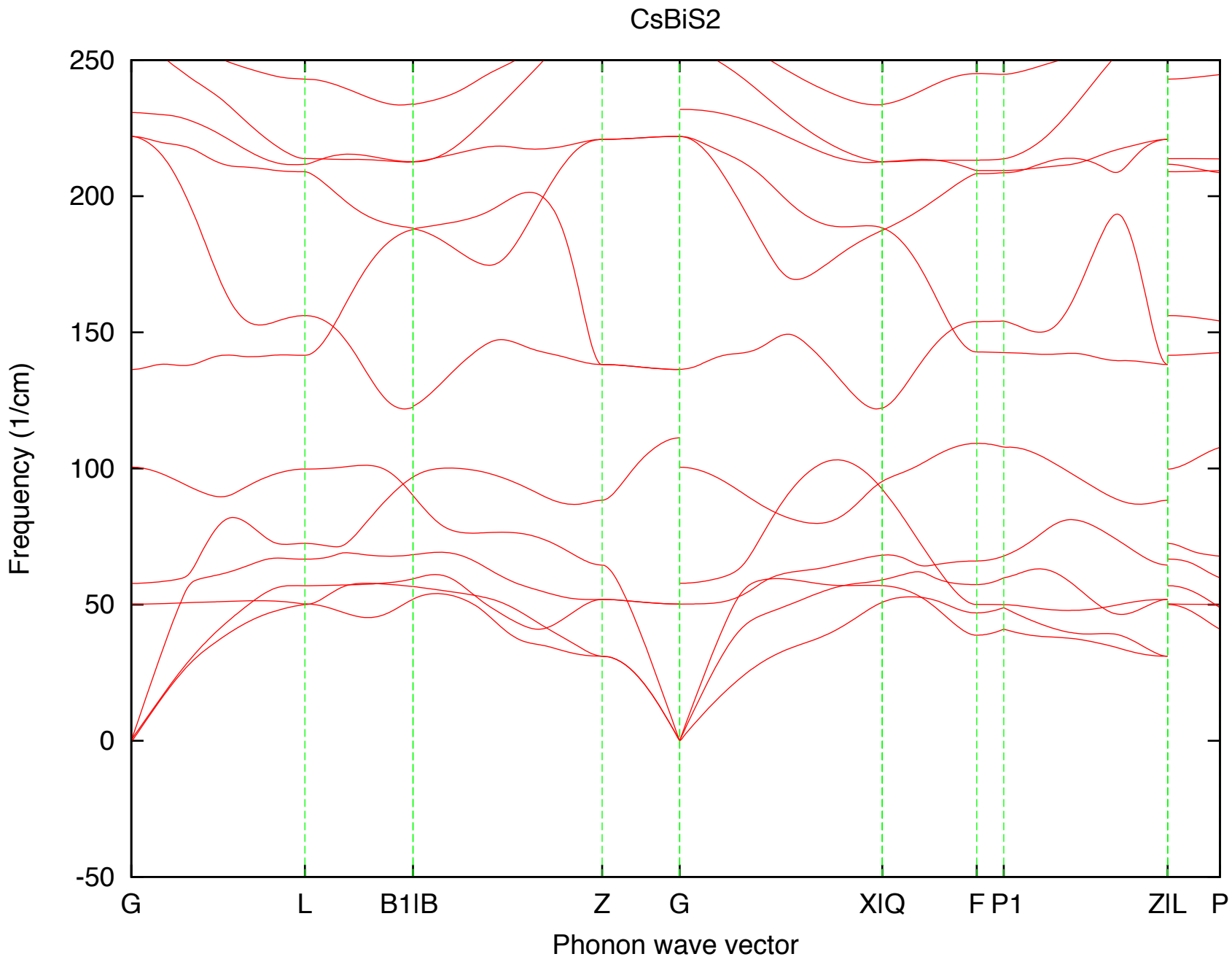
CsBiS2
250
200
150
100
50
0
-50
Frequency (1/cm)
G
L
B1|B
Z
G
X|Q
F
P1
Z|L
P
Phonon wave vector

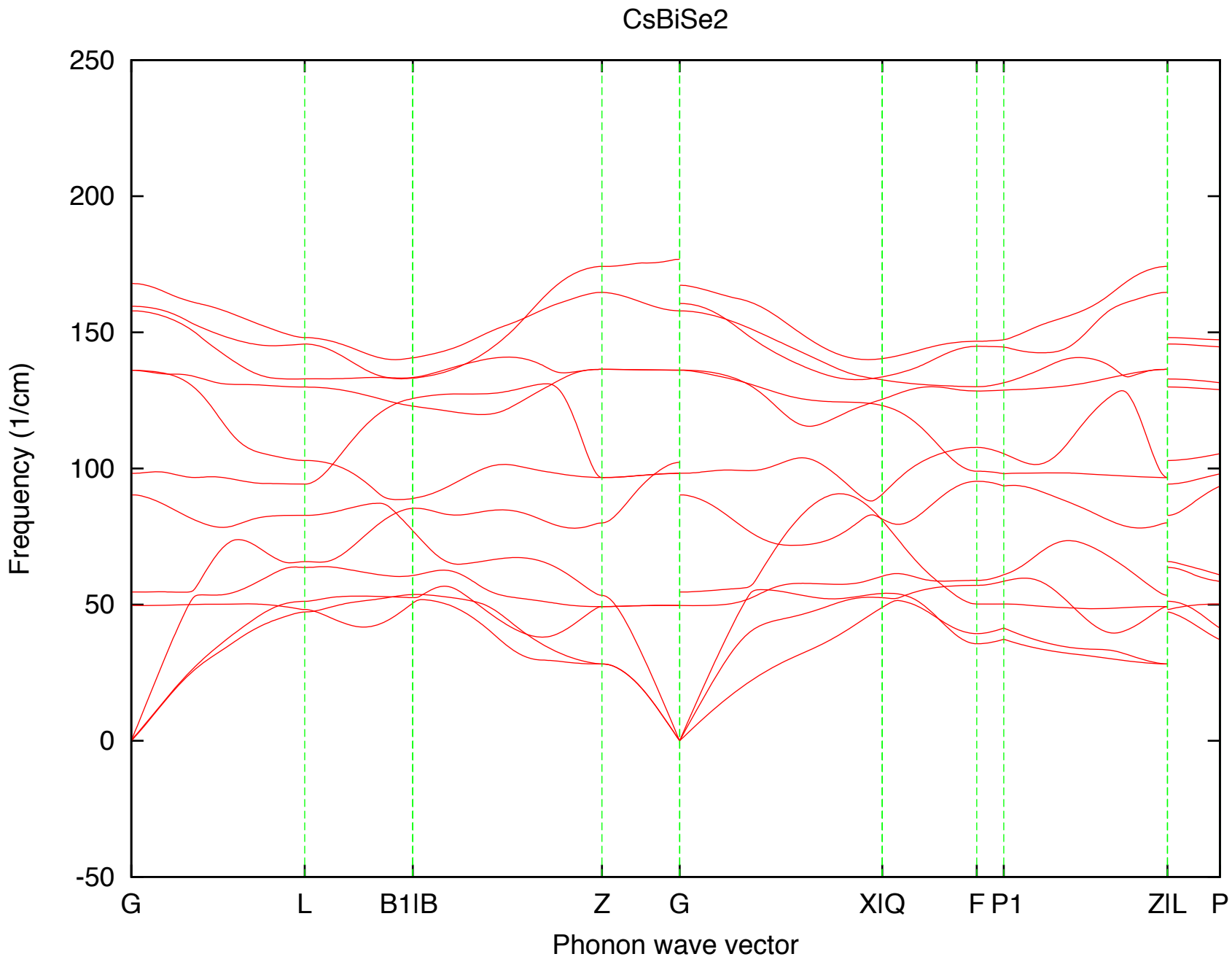
CsBiSe2
250
200
150
100
50
0
-50
Frequency (1/cm)
G
L
B1|B
Z
G
X|Q
F
P1
Z|L
P
Phonon wave vector

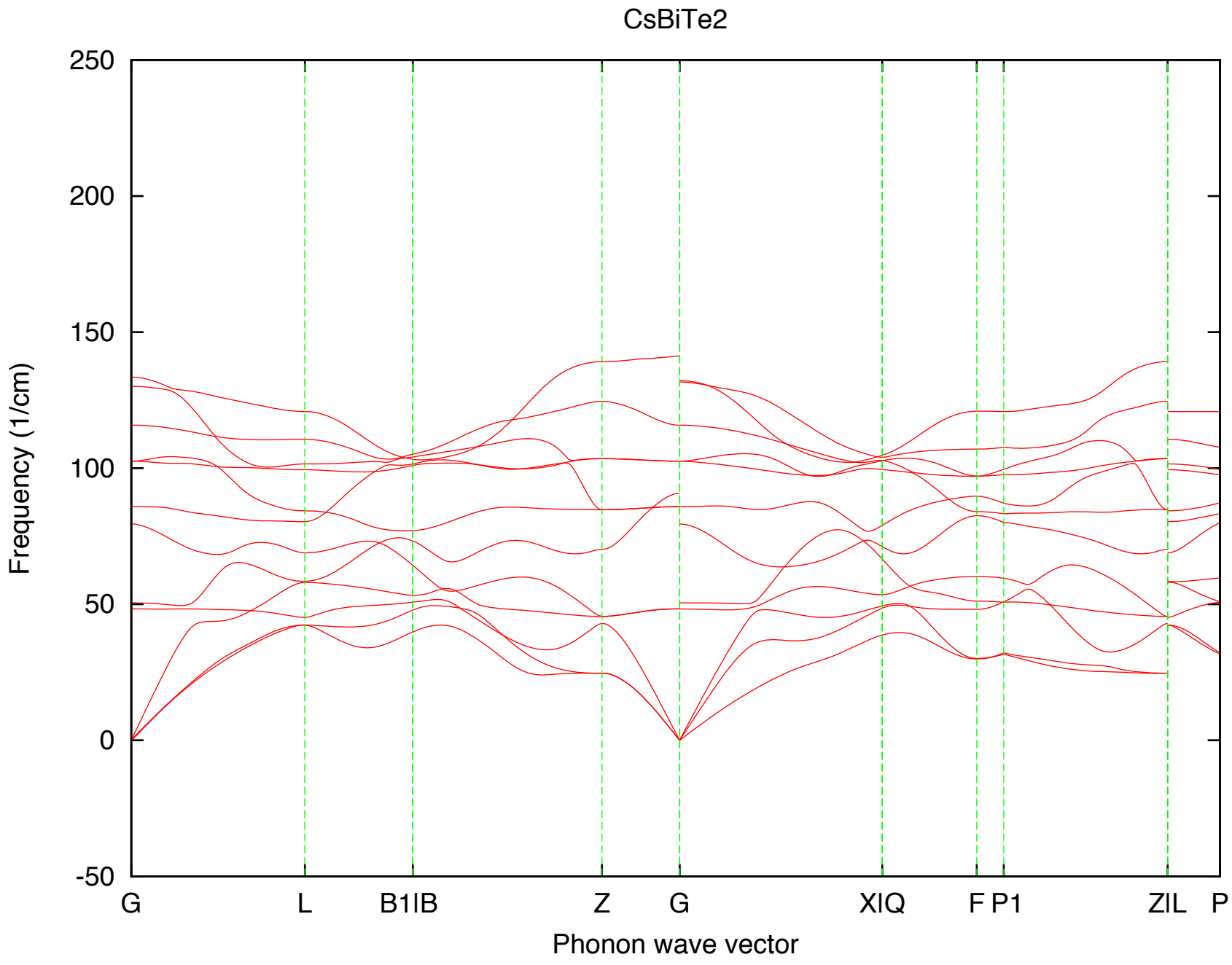
CsBiTe2
250
200
150
100
50
0
-50
Frequency (1/cm)
G
L
B1|B
Z
G
X|Q
F
P1
Z|L
P
Phonon wave vector

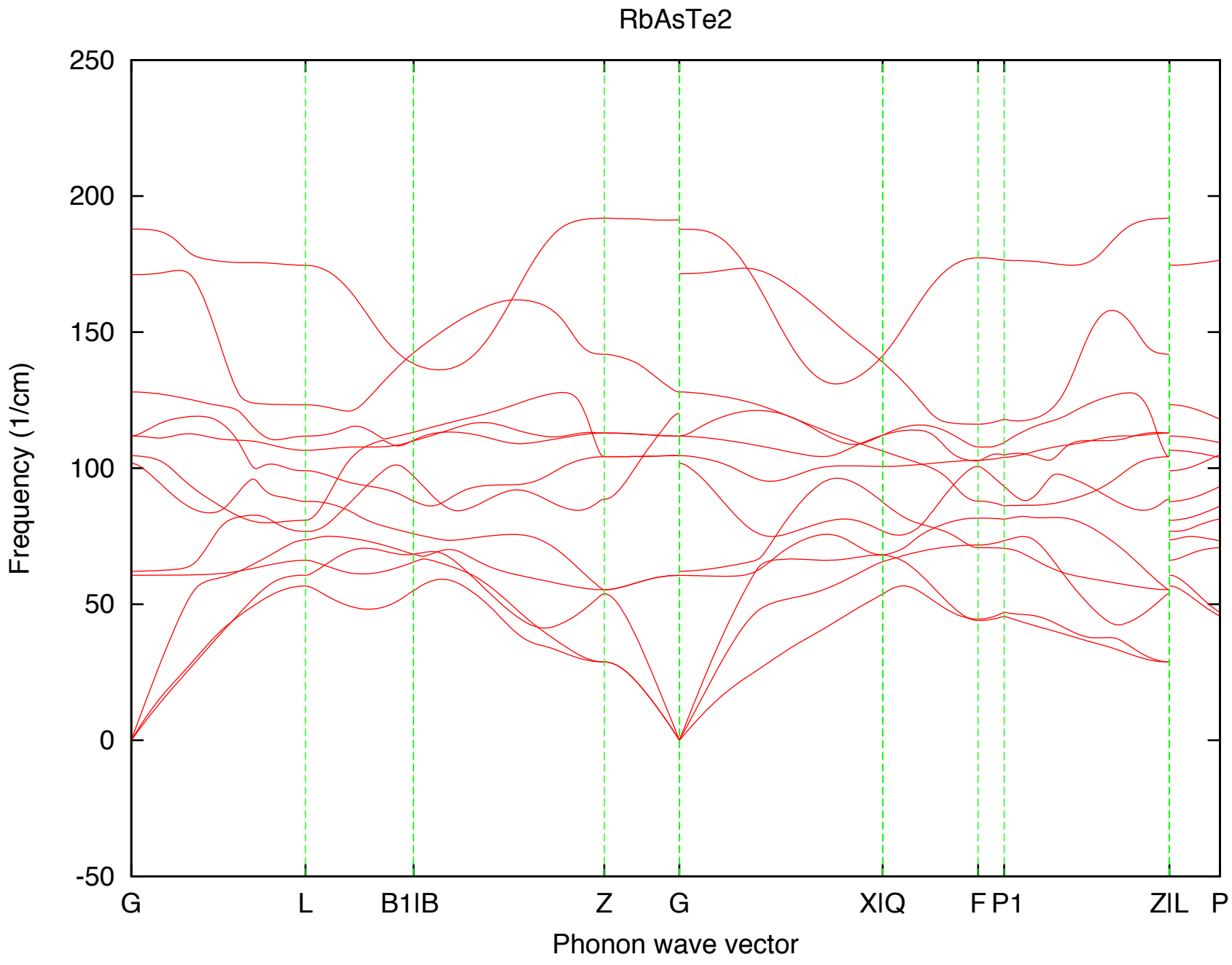

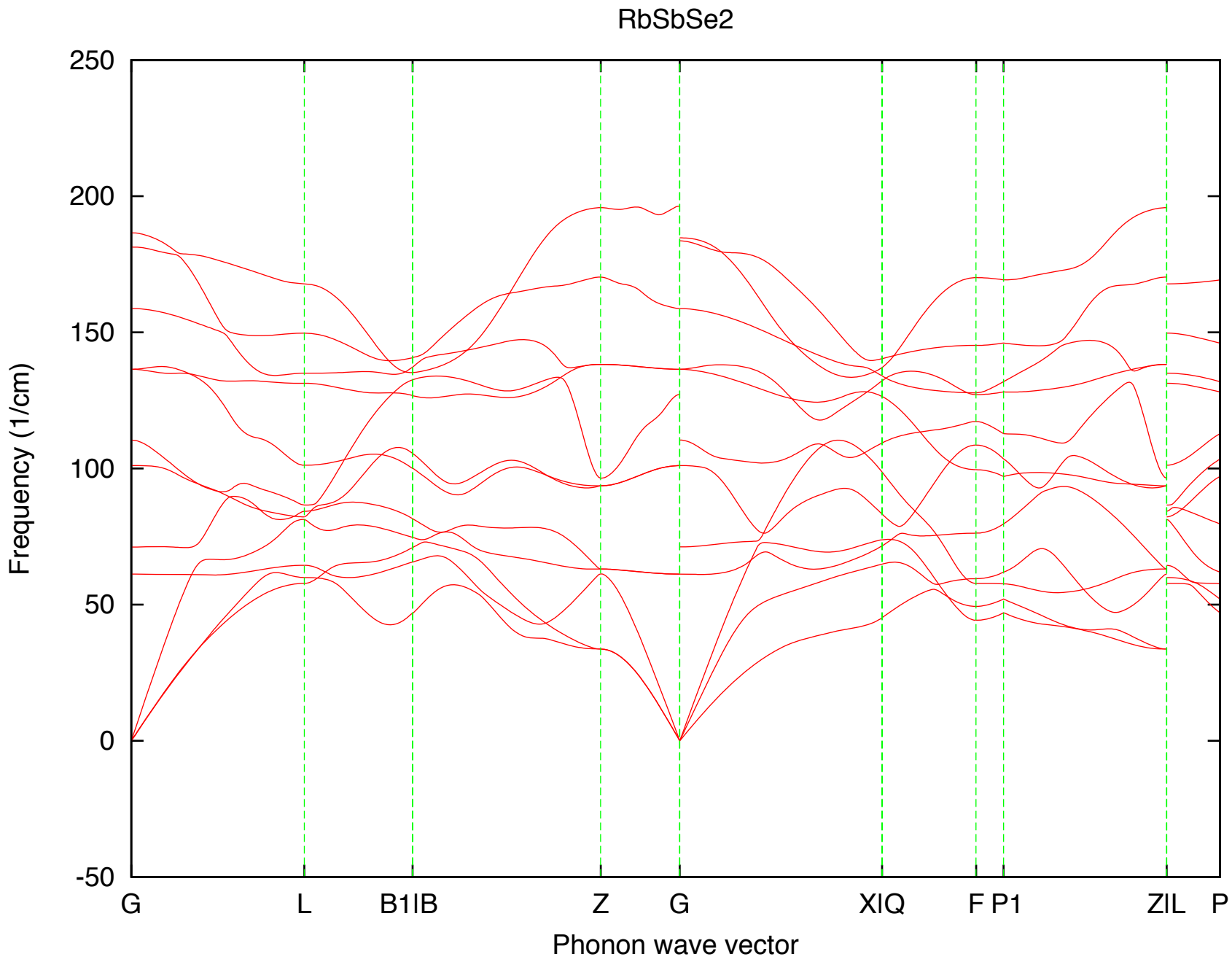
RbSbSe2
250
200
150
100
50
0
-50
Frequency (1/cm)
G
L
B1|B
Z
G
X|Q
F
P1
Z|L
P
Phonon wave vector

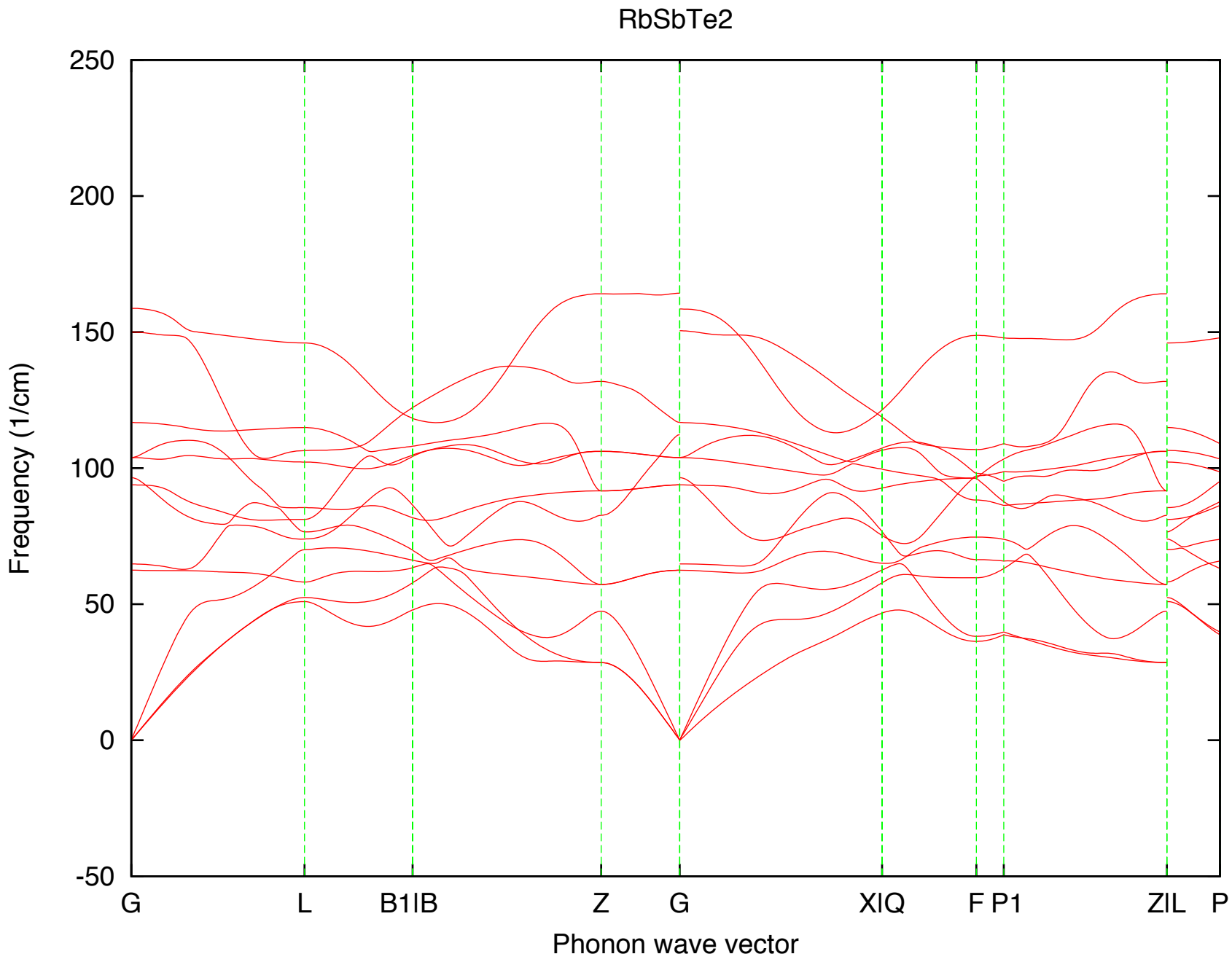
RbSbTe2
250
200
150
100
50
0
-50
Frequency (1/cm)
G
L
B1|B
Z
G
X|Q
F
P1
Z|L
P
Phonon wave vector

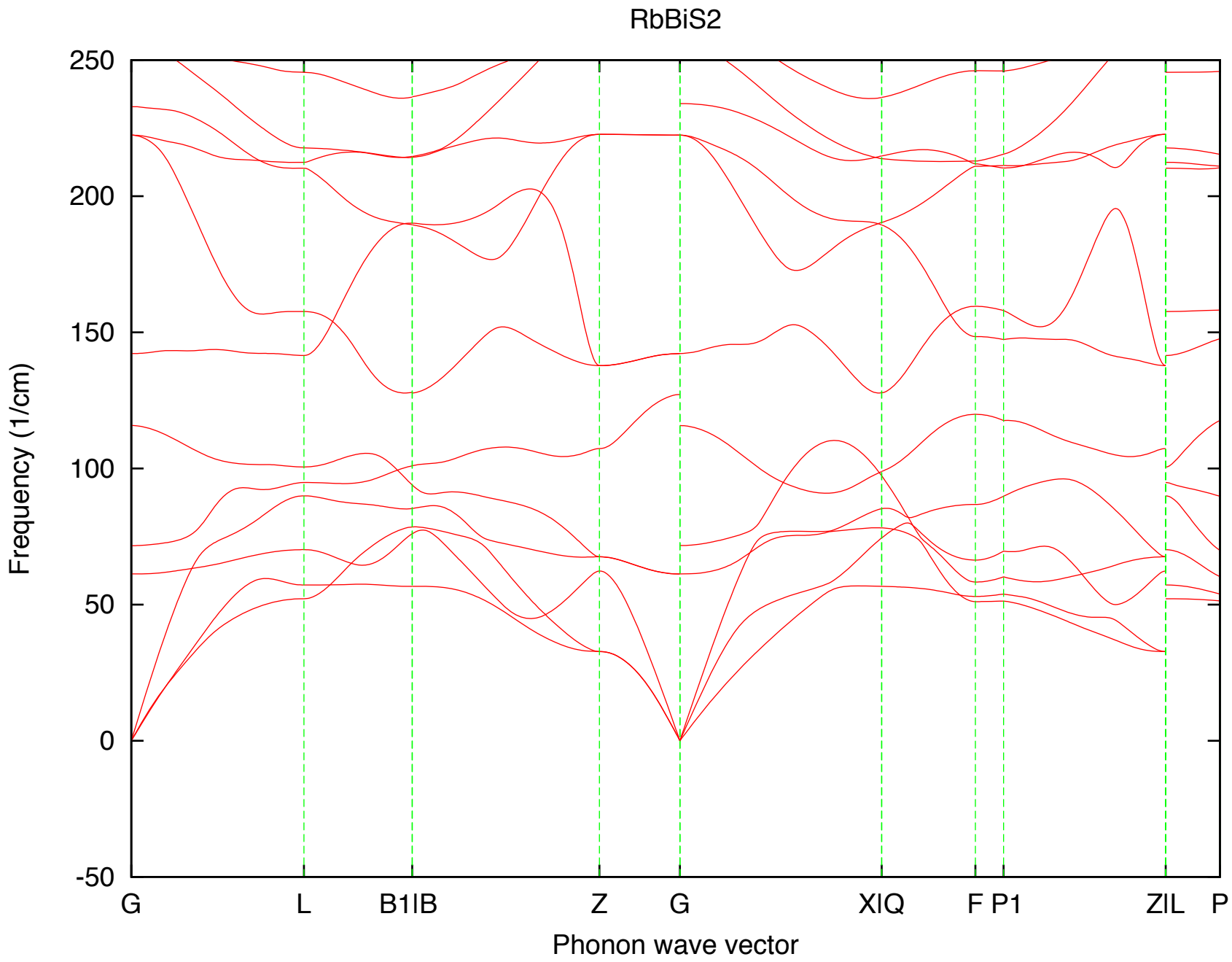
RbBiS2
250
200
150
100
50
0
-50
Frequency (1/cm)
G
L
B1|B
Z
G
X|Q
F
P1
Z|L
P
Phonon wave vector

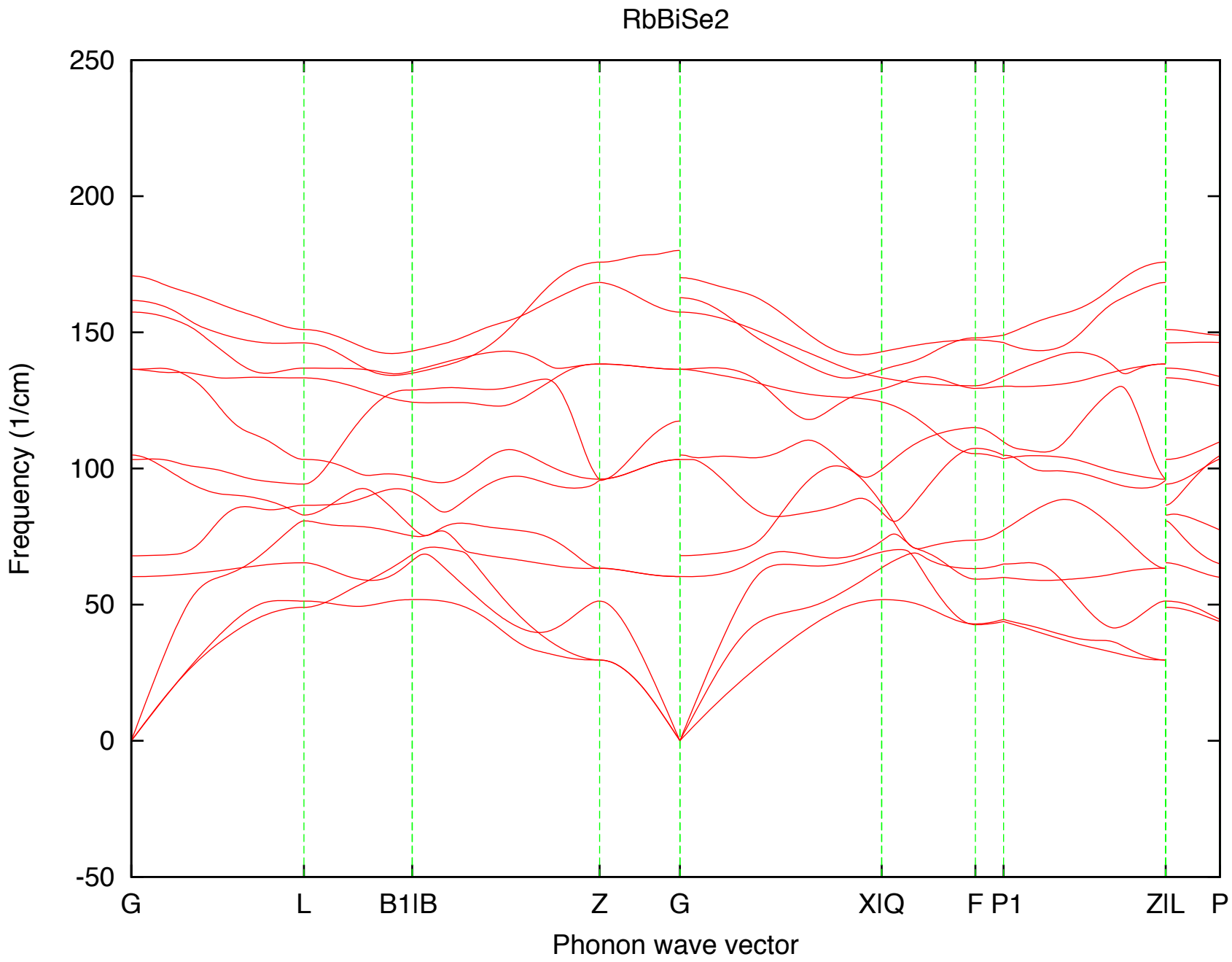
RbBiSe2
250
200
150
100
50
0
-50
Frequency (1/cm)
G
L
B1|B
Z
G
X|Q
F
P1
Z|L
P
Phonon wave vector

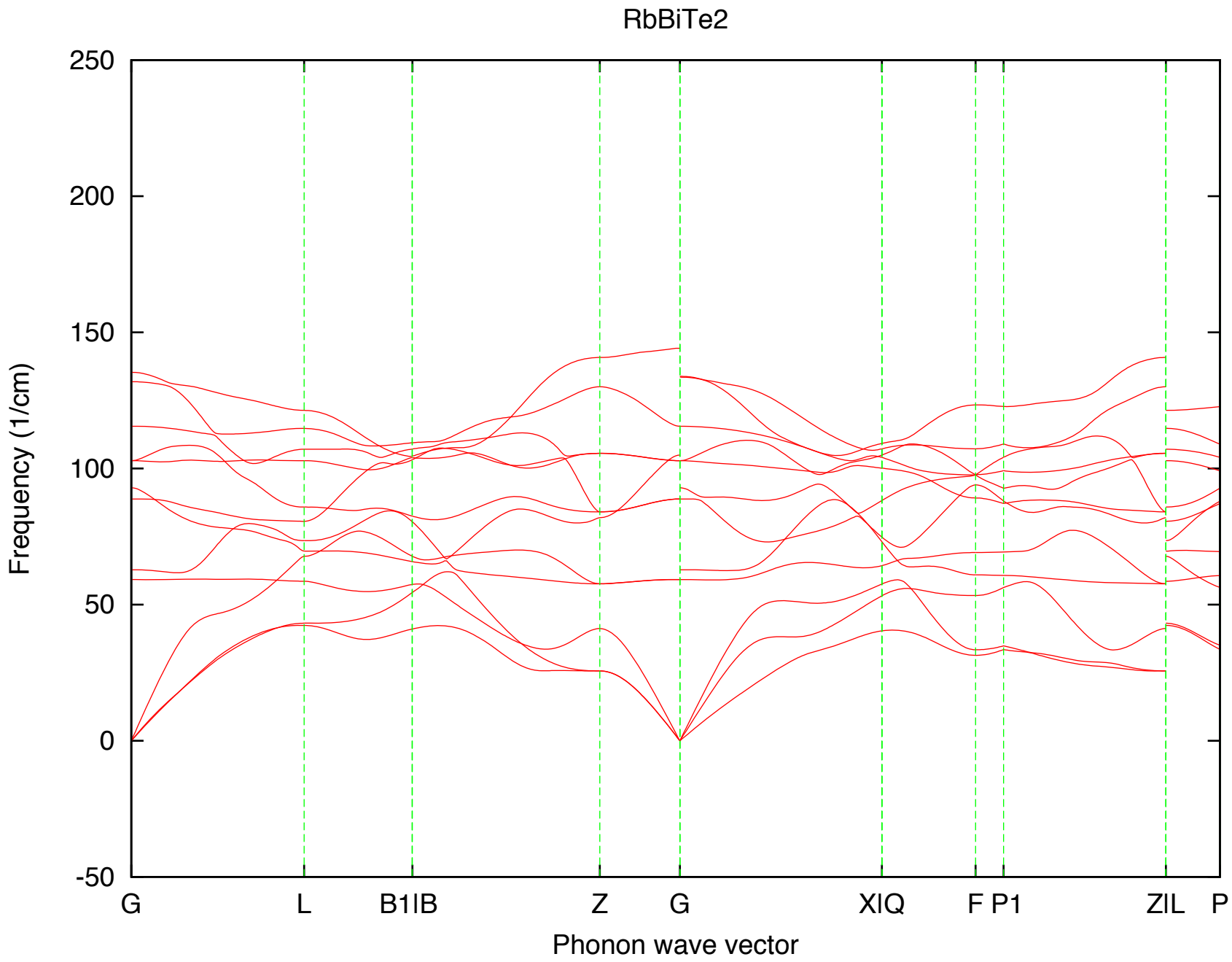
RbBiTe2
250
200
150
100
50
0
-50
Frequency (1/cm)
G
L
B1|B
Z
G
X|Q
F
P1
Z|L
P
Phonon wave vector

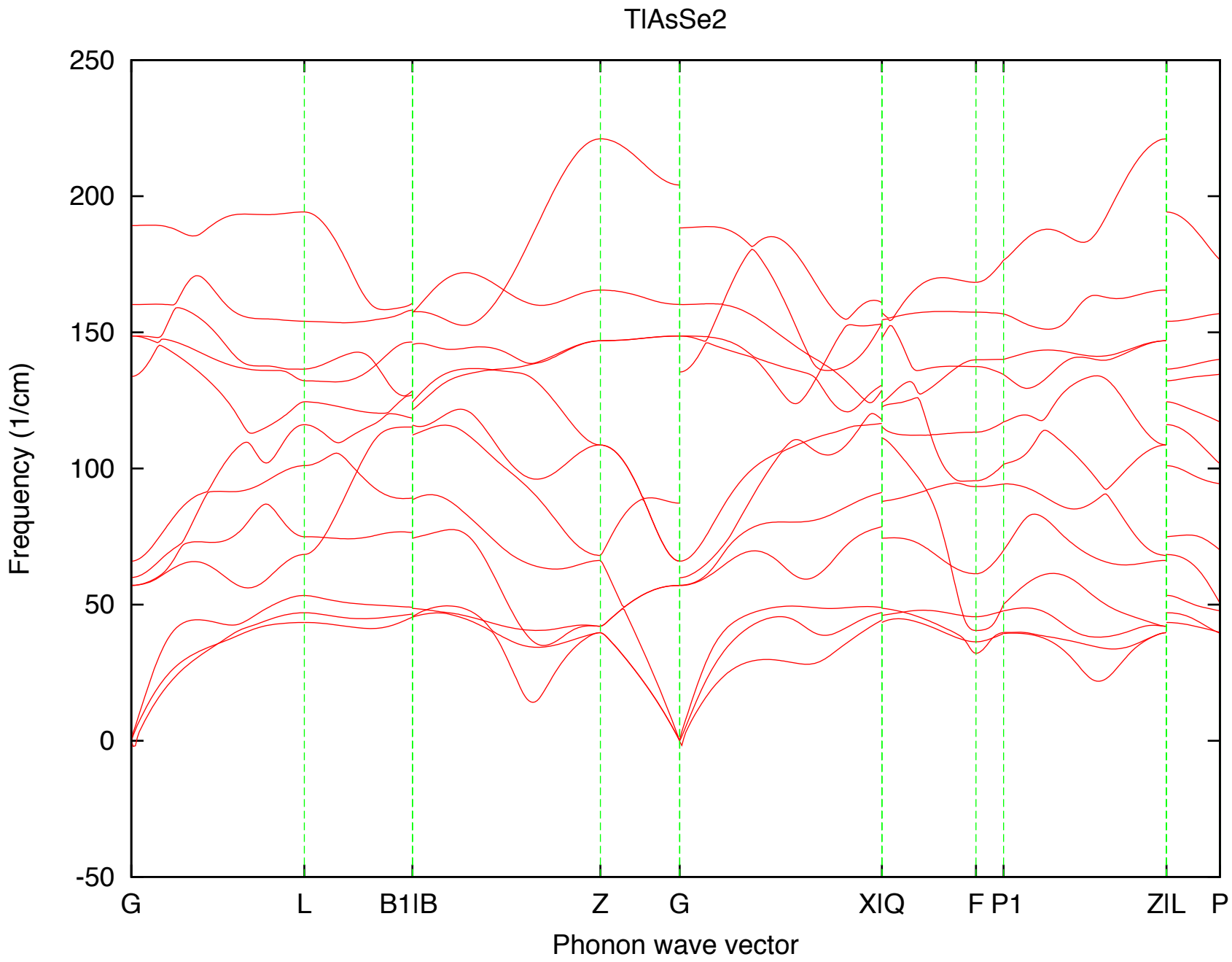
TlAsSe2
250
200
150
100
50
0
-50
Frequency (1/cm)
G
L
B1|B
Z
G
X|Q
F
P1
Z|L
P
Phonon wave vector

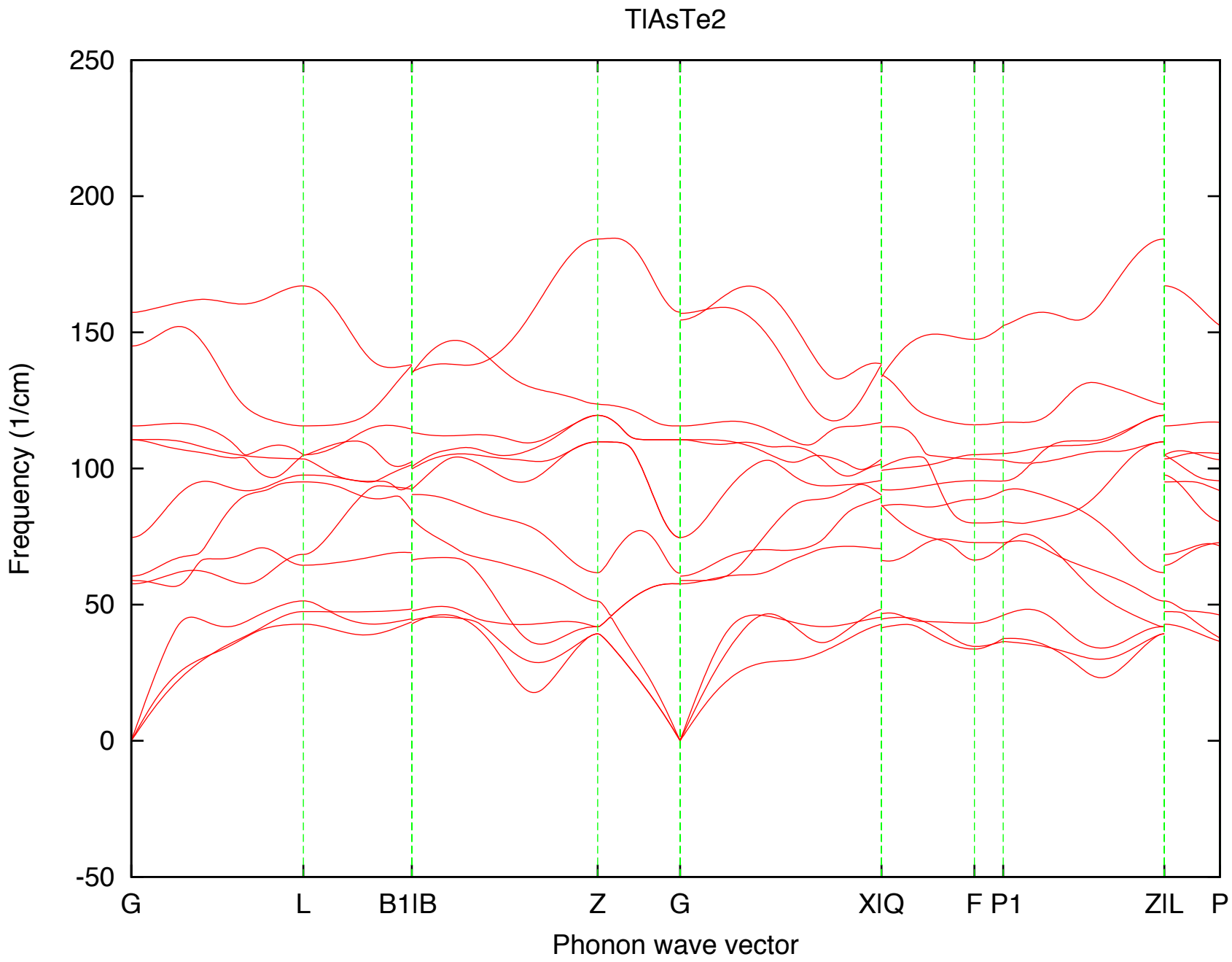
TlAsTe2
250
200
150
100
50
0
-50
Frequency (1/cm)
G
L
B1|B
Z
G
X|Q
F
P1
Z|L
P
Phonon wave vector

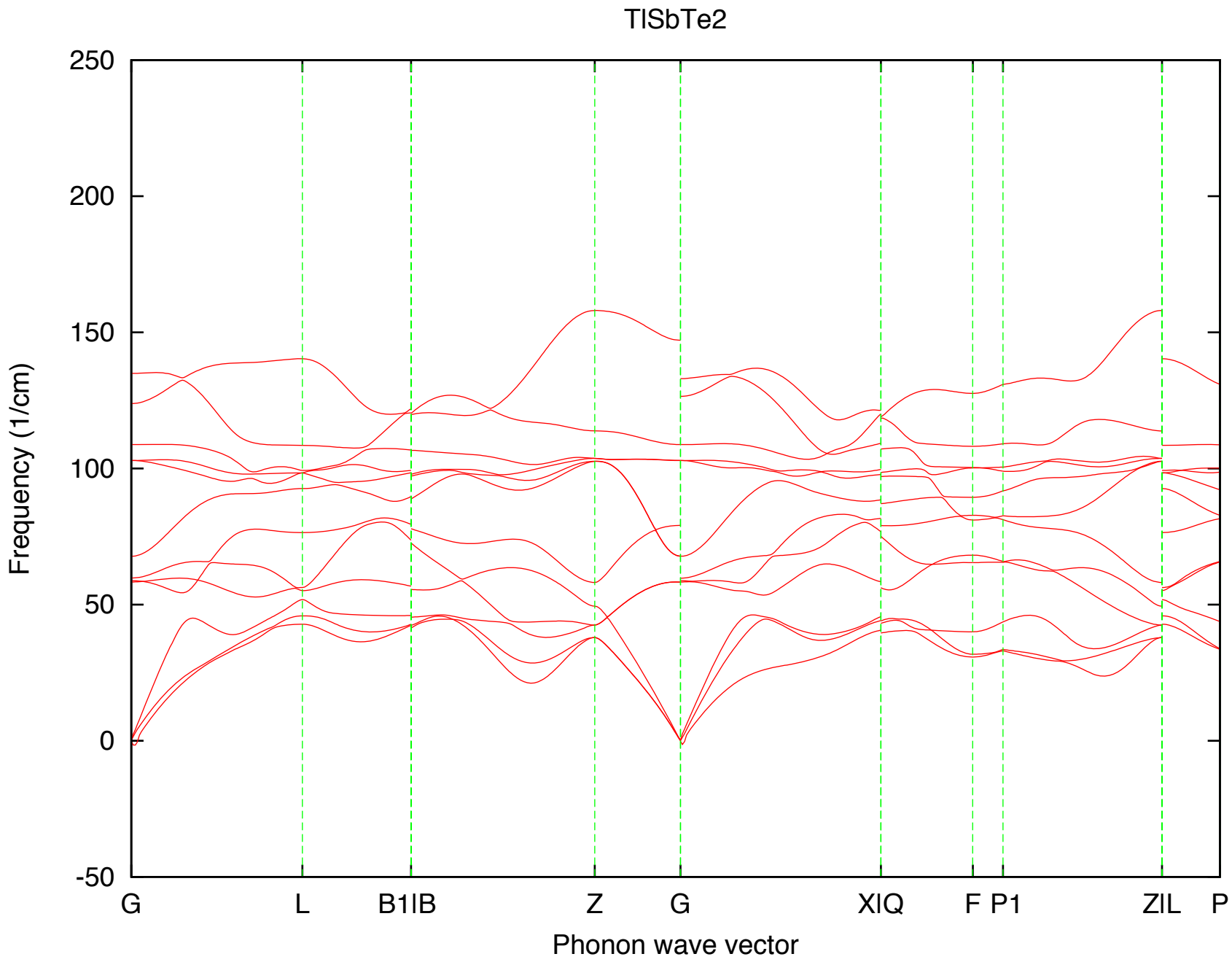
TlSbTe2
250
200
150
100
50
0
-50
Frequency (1/cm)
G
L
B1|B
Z
G
X|Q
F
P1
Z|L
P
Phonon wave vector

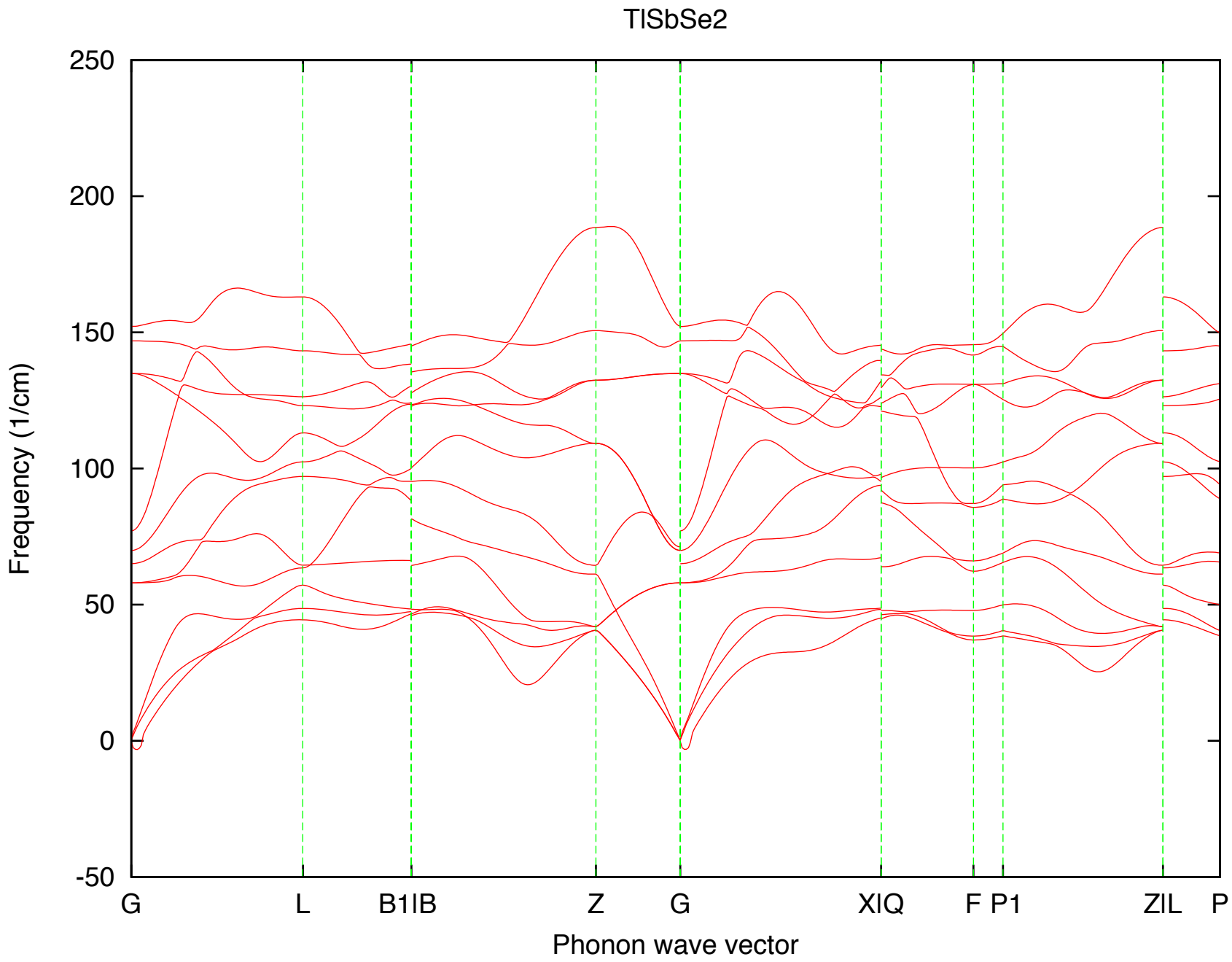
TlSbSe2
250
200
150
100
50
0
-50
Frequency (1/cm)
G
L
B1|B
Z
G
X|Q
F
P1
Z|L
P
Phonon wave vector

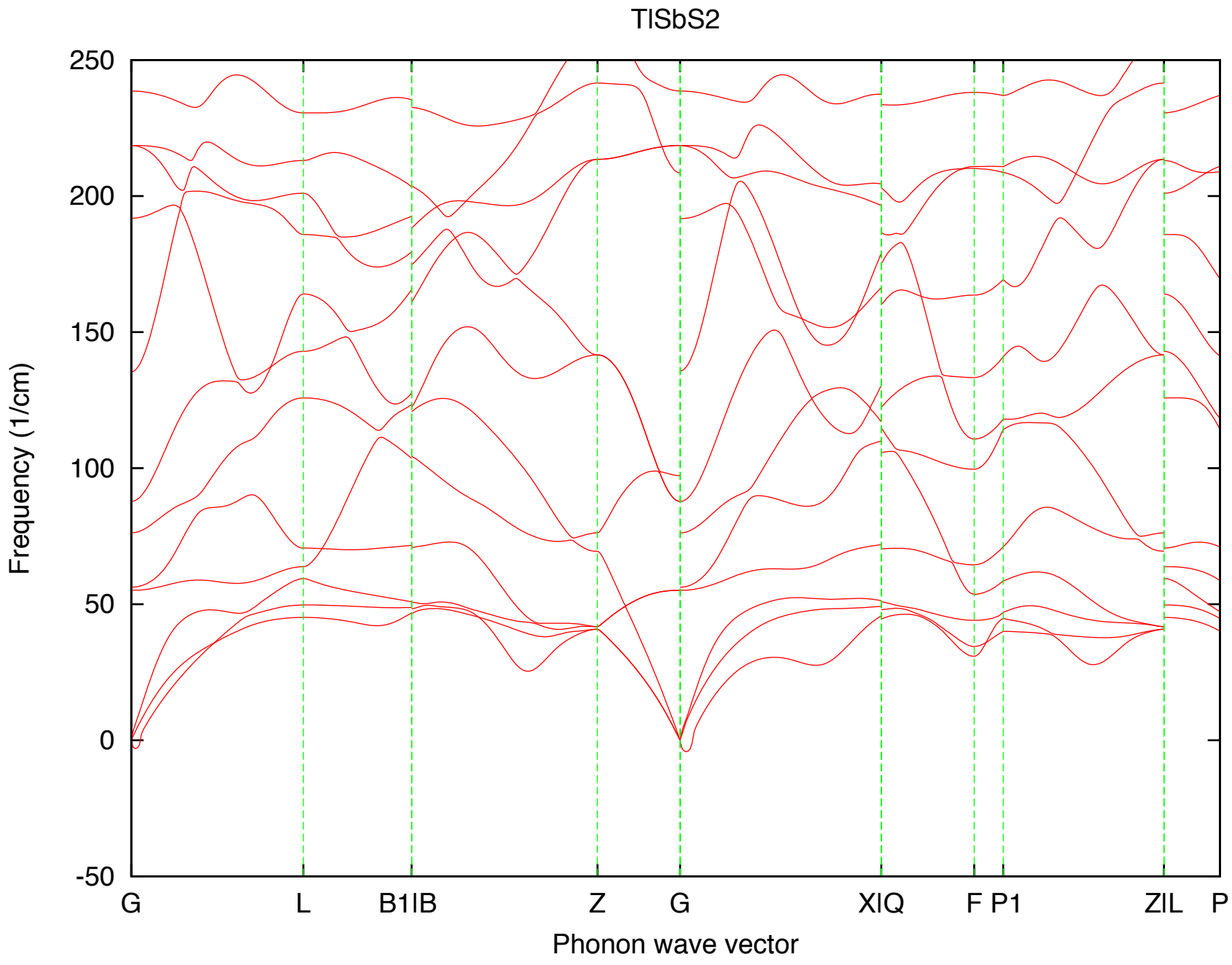
TlSbS2
250
200
150
100
50
0
-50
Frequency (1/cm)
G
L
B1|B
Z
G
X|Q
F
P1
Z|L
P
Phonon wave vector

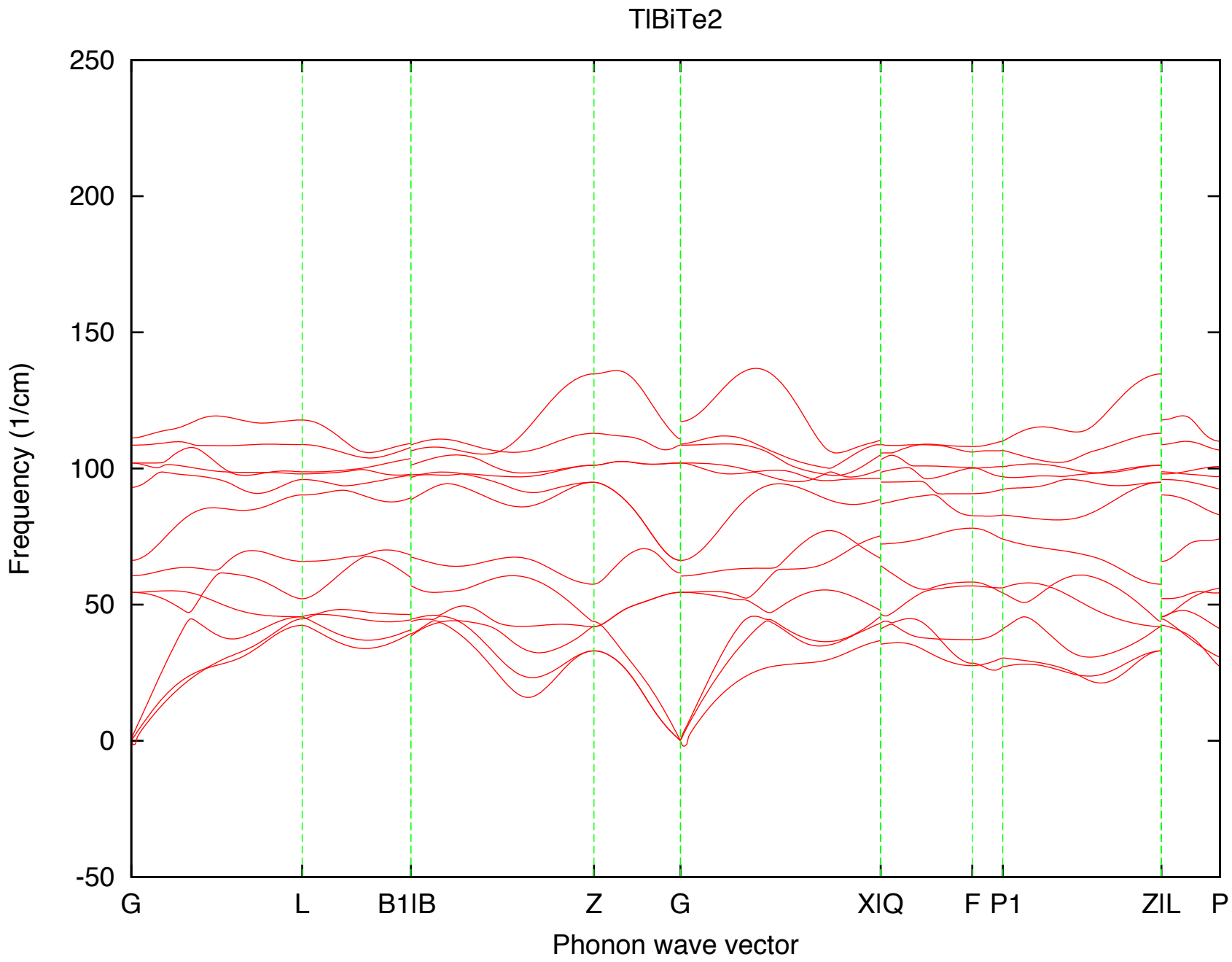
TlBiTe2
250
200
150
100
50
0
-50
Frequency (1/cm)
G
L
B1|B
Z
G
X|Q
F
P1
Z|L
P
Phonon wave vector

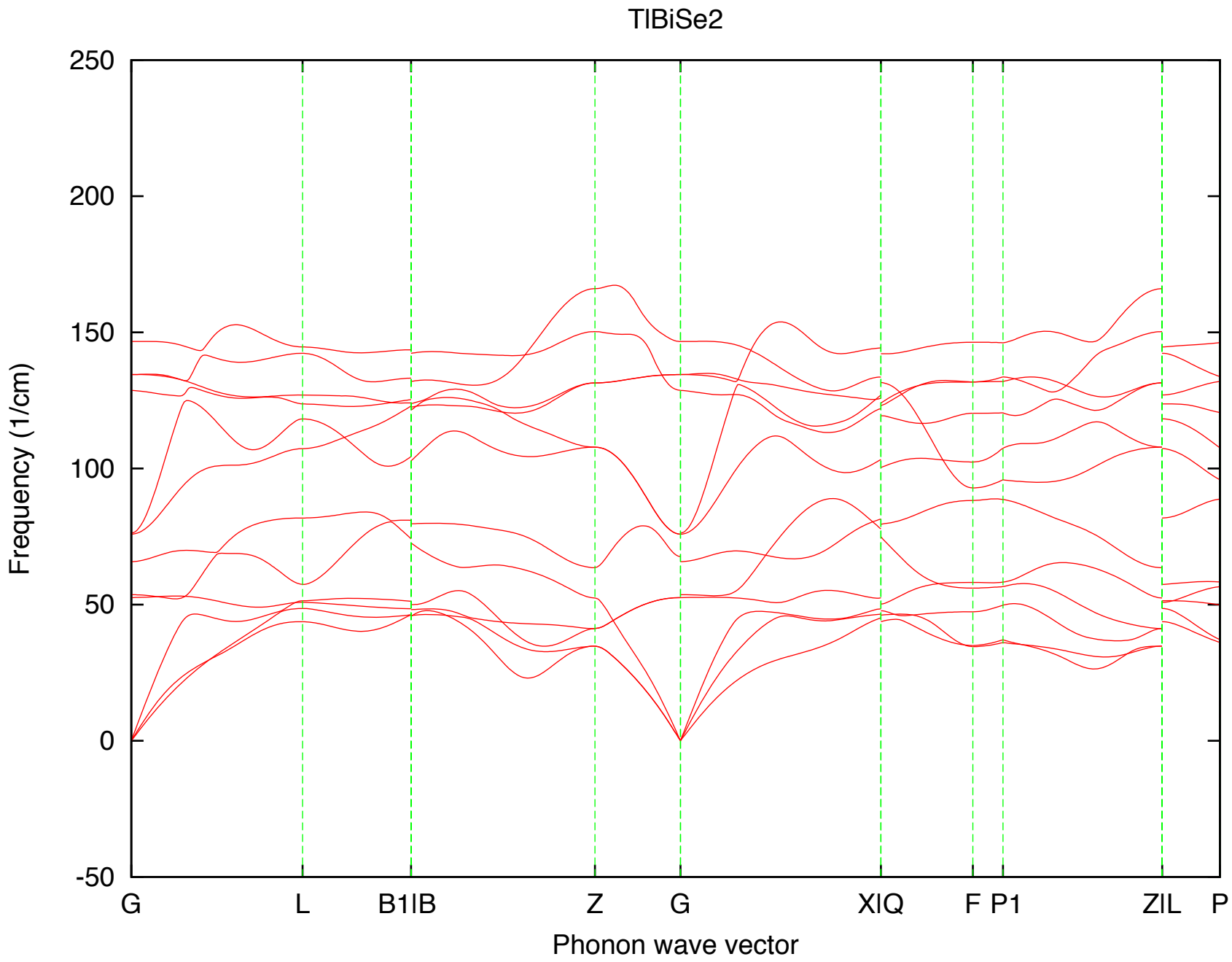
TlBiSe2
250
200
150
100
50
0
-50
Frequency (1/cm)
G
L
B1|B
Z
G
X|Q
F
P1
Z|L
P
Phonon wave vector

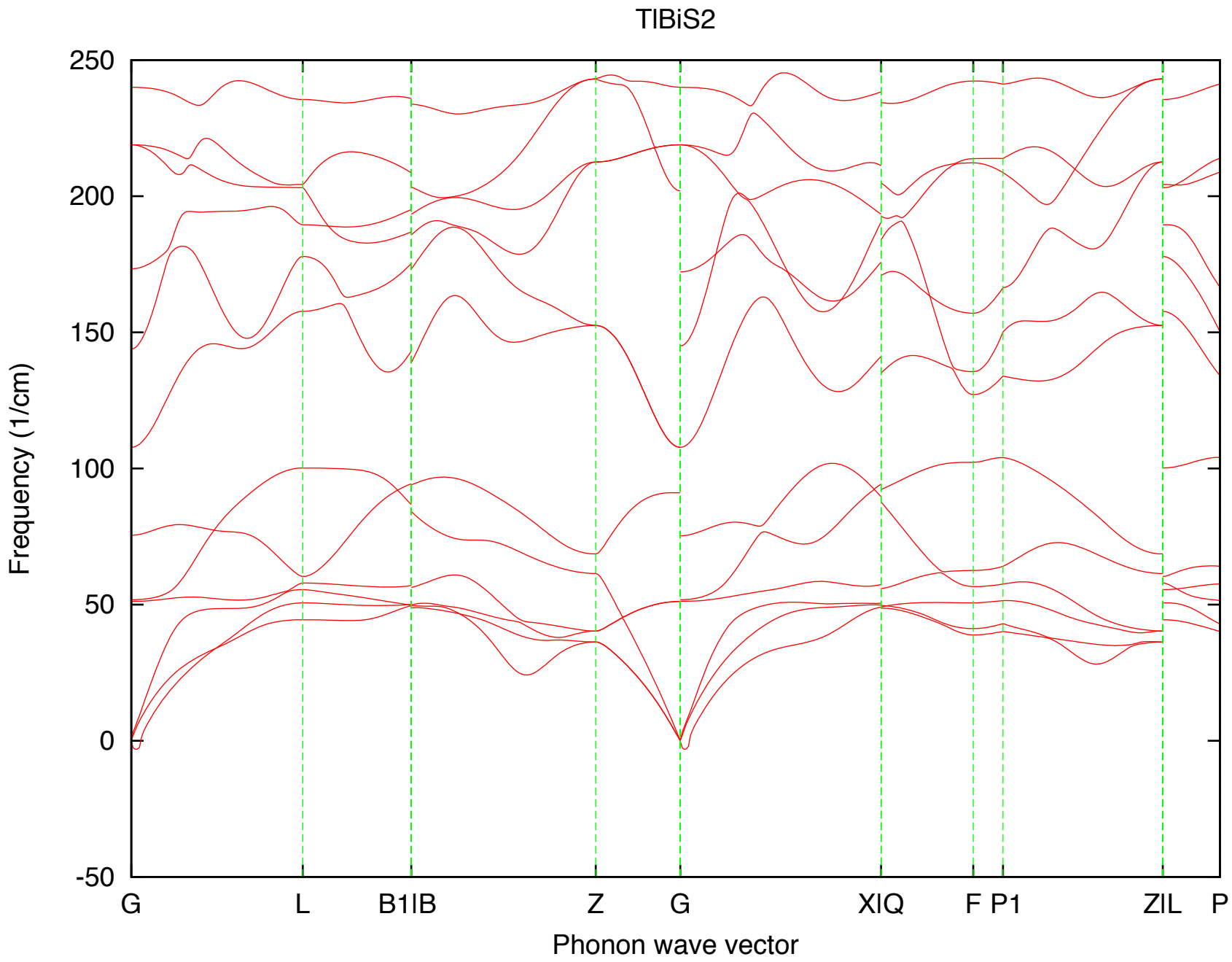
TlBiS2
250
200
150
100
50
0
-50
Frequency (1/cm)
G
L
B1|B
Z
G
X|Q
F
P1
Z|L
P
Phonon wave vector